Materials Today Bio 12 (2021) 100173

Contents lists available at ScienceDirect

Materials Today Bio

journal homepage: www.journals.elsevier.com/materials-today-bio

Layer-specific stem cell differentiation in tri-layered tissue engineering biomaterials: Towards development of a single-stage cell-based approach for osteochondral defect repair

Tanya J. Levingstone [a,b,c,d,e,f,1], Conor Moran [a,e,f,1], Henrique V. Almeida [e,g,h,i], Daniel J. Kelly [b,f,i], Fergal J. O'Brien [a,e,f,*]

[a] Tissue Engineering Research Group, Department of Anatomy and Regenerative Medicine, Royal College of Surgeons in Ireland (RCSI), 123 St. Stephen's Green, Dublin, 2, Ireland
[b] School of Mechanical and Manufacturing Engineering, Dublin City University, Dublin, 9, Ireland
[c] Centre for Medical Engineering Research (MEDeng), Dublin City University, Dublin, 9, Ireland
[d] Advanced Processing Technology Research Centre, Dublin City University, Dublin, 9, Ireland
[e] Trinity Centre for Bioengineering, Trinity Biomedical Sciences Institute, Trinity College Dublin, Dublin, 2, Ireland
[f] Advanced Materials and Bioengineering Research (AMBER) Centre, RCSI & TCD, Ireland
[g] iBET, Instituto de Biologia Experimental e Tecnológica, 2781-901, Oeiras, Portugal
[h] Instituto de Tecnologia Química e Biológica António Xavier, Universidade Nova de Lisboa, 2780-157, Oeiras, Portugal
[i] Department of Mechanical and Manufacturing Engineering, School of Engineering, Trinity College Dublin, Dublin, 2, Ireland

ARTICLE INFO

Keywords:
Osteochondral
Tissue engineering
In vitro
Cartilage
Cell-seeding

ABSTRACT

Successful repair of osteochondral defects is challenging, due in part to their complex gradient nature. Tissue engineering approaches have shown promise with the development of layered scaffolds that aim to promote cartilage and bone regeneration within the defect. The clinical potential of implanting these scaffolds cell-free has been demonstrated, whereby cells from the host bone marrow MSCs infiltrate the scaffolds and promote cartilage and bone regeneration within the required regions of the defect. However, seeding the cartilage layer of the scaffold with a chondrogenic cell population prior to implantation may enhance cartilage tissue regeneration, thus enabling the treatment of larger defects. Here the development of a cell seeding approach capable of enhancing articular cartilage repair without the requirement for *in vitro* expansion of the cell population is explored. The intrinsic ability of a tri-layered scaffold previously developed in our group to direct stem cell differentiation in each layer of the scaffold was first demonstrated. Following this, the optimal chondrogenic cell seeding approach capable of enhancing the regenerative capacity of the tri-layered scaffold was demonstrated with the highest levels of chondrogenesis achieved with a co-culture of rapidly isolated infrapatellar fat pad MSCs (FPMSCs) and chondrocytes (CCs). The addition of FPMSCs to a relatively small number of CCs led to a 7.8-fold increase in the sGAG production over chondrocytes in mono-culture. This cell seeding approach has the potential to be delivered within a single-stage approach, without the requirement for costly *in vitro* expansion of harvested cells, to achieve rapid repair of osteochondral defects.

1. Introduction

Osteochondral tissue is composed of articular cartilage and the underlying subchondral bone, anchored together with a calcified cartilage layer. The gradient nature of the tissue and poor intrinsic regenerative properties of cartilage tissue makes the repair of osteochondral lesions challenging. Current best clinical practice for the treatment of such lesions involves the use of autologous grafts harvested from non load-bearing regions within the joint that are implanted into the defect site e.g. mosaicplasty. This approach has limitations including the lack of availability of suitable graft tissue, donor site morbidity and poor long-term repair outcomes [1,2]. Long-term failure following mosaicplasty

* Corresponding author. Tissue Engineering Research Group, Department of Anatomy and Regenerative Medicine, Royal College of Surgeons in Ireland (RCSI), 123 St. Stephen's Green, Dublin, 2, Ireland.
E-mail address: fjobrien@rcsi.ie (F.J. O'Brien).
[1] Authors contributed equally.

https://doi.org/10.1016/j.mtbio.2021.100173
Received 22 September 2021; Received in revised form 25 November 2021; Accepted 27 November 2021
Available online 27 November 2021

osteochondral autograft transfer is reportedly 51% with a mean time to failure of 8.4 years [2]. Thus, it is imperative to develop new approaches to treat this clinical challenge.

Recently tissue engineering approaches have shown some promise whereby biomaterial scaffolds, cells and signalling factors are combined in order to promote tissue regeneration. Specifically for osteochondral tissue engineering, there has been a focus on the development of layered scaffolds that aim to promote cartilage and bone regeneration within the requisite regions of the defect site [3–6]. Within our lab, we have developed a tri-layered scaffold for osteochondral defect repair consisting of cartilage, bone and intermediate regions (Fig. 1) [4]. This highly porous scaffold (>98.8% porosity) has a seamlessly integrated layer structure that enables cellular infiltration throughout the scaffold. The layers of the scaffold have been tailored in terms of their composition, architecture and mechanical properties to mimic the native tissues and promote the formation of bone, cartilage and an intermediate 'tidemark' layer to form a boundary between the two regions and thus prevent bony overgrowth into the cartilage region which commonly occurs during osteochondral defect repair [7]. The scaffold has a compressive modulus of 0.51 kPa and average pore diameters of 126 μm, 112 μm and 136 μm in the cartilage, intermediate and bone layer scaffolds respectively [4]. Full characterisation of this scaffold has been previously reported [4]. This biomimetic tri-layered scaffold has shown success *in vivo* as an off-the-shelf cell-free scaffold in focal defects in a rabbit medial femoral condyle model at 3 months post implantation [8], in goat medial femoral condyle and lateral trochlear ridge models at 12 months post implantation [9], and clinically in an equine case study for the treatment of bi-lateral osteochondritis dissecans [10]. The scaffold recruits host cells from the bone marrow and directs them to form bone and cartilage in the requisite layers, with restoration of the anatomical tidemark, resulting in joint regeneration.

While a rich supply of bone marrow MSCs is available from within the bone marrow cavity beneath the subchondral bone, chondrocytes (CCs) are present at a low density within the native cartilage making up only 1.7% of the cartilage matrix, with a corresponding numerical density of roughly 1800 per mm^3 [11]. Furthermore, they have a reduced ability to migrate into a scaffold as they are embedded within a dense matrix of proteoglycans and collagen [12]. Thus, seeding the cartilage region of the scaffolds with a chondrogenic cell population prior to implantation may present an improved approach to enhance the regeneration of the cartilage tissue, leading to more rapid repair of cartilage tissue and enabling the treatment of larger defects. Recently the potential of cell-seeded scaffolds for the promotion of osteochondral defect repair has been demonstrated [13,14] although to date neither the ideal cell seeding approach nor ideal cell type, has been determined. While chondrocytes represent the most obvious cell choice for cartilage tissue engineering applications, their low density generally requires a two-stage procedure whereby cells are harvested during the initial procedure and then expanded *in vitro* prior to re-implantation in a second stage procedure [12,15]. This approach is currently used clinically in both autologous chondrocyte implantation (ACI) and matrix-assisted ACI (MACI) techniques. Limitations of these approaches include the cost associated with the two-stage procedure, and the costs and risk of chondrocyte dedifferentiation associated with *in vitro* chondrocyte expansion. In order to circumvent these issues a wide range of alternative cell types have been investigated, including bone marrow MSCs (BMMSCs), infrapatellar fat pad MSCs (FPMSCs), nasal chondrocytes, human embryonic stem cells (hESCs), induced pluripotent stem cells (iPSCs), adipose-derived stem cells (ADSCs) and allogenic chondrocytes [16–21]. BMMSCs and FPMSCs have shown particular potential for cartilage repair as they are readily available in large numbers [22–28], and in addition, they demonstrate immunomodulatory effects which can enhance tissue repair [29,30]. Currently, BMMSCs are used to stimulate cartilage repair in the microfracture technique, where the surgeon creates small drill holes in the subchondral bone to stimulate BMMSC release into the defect site. When larger cell numbers are required, BMMSCs are accessed from a secondary location, such as the iliac crest. This second surgical site, however, can add a further risk of infection and required increased surgical time [31]. FPMSCs have been proven to be an abundant source of cells that can be easily harvested at diagnostic arthroscopy without causing morbidity to

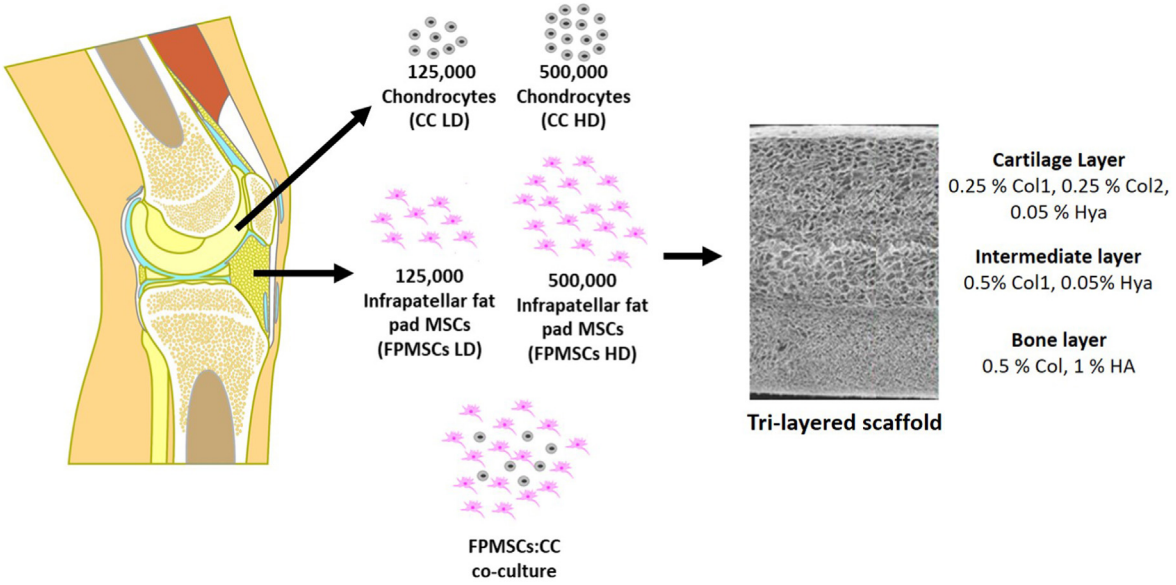

Fig. 1. Tri-layered scaffolds consisting on a cartilage layer, intermediate layer and bone layer are seeded with chondrocytes (CCs), infrapatellar fat pad MSCs (FPMSCs) at low and high density and a co-culture of CCs and FPMSCs.

the patient, thereby avoiding the requirement for multiple invasive procedures [32,33]. FPMSCs have been shown to retain their chondrogenic potential, even in the diseased state, and the safety and suitability of FPMSCs from OA patients has been proven *in vitro* and in clinical studies [25]. This is clinically important for patients who may present late with osteochondral defects that already show evidence of osteoarthritic changes. Furthermore, FPMSCs have shown a higher capacity for chondrogenic differentiation than MSCs from body fat, bone marrow, synovial membrane and Wharton's jelly of the umbilical cord [27,34]. Recent research has demonstrated the potential of co-cultures of CCs and MSCs for the treatment of cartilage defects. This co-culture approach has been shown to achieve increased cartilage matrix production *in vitro* over CCs and MSCs mono-cultures [35–40].

Within this study, we explored the development of a cell seeding approach that would provide a cell-seeded scaffold capable of achieving articular cartilage repair without the requirement for *in vitro* expansion of the cell population. In order to achieve this goal, the ability of the intrinsic properties of the scaffold to direct stem cell differentiation in each layer of the scaffold was first explored. Following this, the optimal chondrogenic cell source capable of enhancing the regenerative capacity of the tri-layered scaffold was investigated. To this end, the scaffolds were seeded with rapidly isolated CCs, FPMSCs and a co-culture of FPMSCs and CCs and the ability of the different cell combinations to support chondrogenesis was investigated.

2. Materials and methods

2.1. Scaffold fabrication

In order to determine the optimal cell-seeding approach each layer of the tri-layered scaffold was first fabricated as individual scaffolds. The bone layer scaffold consisting of 0.5% (w/v) type I microfibrillar bovine tendon collagen (Col1, Collagen Matrix Inc., NJ, USA) and 1% (w/v) hydroxyapatite (HA, Plasma Biotal, CAS No. P288R, Capital R) was fabricated as previously described [4]. Briefly, 1.8 g of microfibrillar bovine tendon collagen was added to 320 ml of 0.5 M acetic acid solution (Fisher Scientific, CAS No. 64-19-7) and blended (15,000 rpm, 4 °C, 90 min) using an overhead blender (Ultra Turrax T18 Overhead Blended, IKA Works Inc., USA). A HA suspension was created by adding 3.6 g of HA to 40 ml of 0.5 M acetic acid solution. This suspension was added to the blended collagen in 10 ml aliquots every 20 min. The entire suspension was then blended for a subsequent hour to obtain a homogenous suspension. Prior to freeze-drying, degassing was carried out in a vacuum chamber (50 mTorr) to removed air introduced during blending. 15.6 ml of the bone layer suspension was pipetted into custom-made stainless steel trays (internal dimensions, 60 mm × 60 mm) and the trays were then placed on the shelves within the freeze-dryer (Virtis Genesis 25 EL, Biopharma, Winchester, UK) and freeze-dried at a constant cooling rate of 1 °C/min to a final freezing temperature of −40 °C and dried under a vacuum pressure of 200 mTorr. Finally, cylindrical scaffold plugs 7 mm in diameter were cut from the scaffold sheet using a biopsy punch.

The intermediate layer scaffold consisting of Col1 [0.5% (w/v)], and hyaluronic acid sodium salt derived from streptococcus equi. (HyA) [0.05% (w/v), Contipro] was fabricated as follows: a hyaluronic acid solution was then made up by adding 0.11 g of hyaluronic acid (hyaluronic acid sodium salt derived from streptococcus equi.) (Sigma-Aldrich, CAS No. 53747-10G) to 40 ml of the 0.5 M acetic acid and stirring for 60 min [4]. 1.2 g of Col1 was then blended with 200 ml of the 0.5 M acetic acid solution (15,000 rpm, 4 °C). The hyaluronic acid solution was added dropwise to the blending collagen to avoid clumping. The slurry was blended for a further 60 min until homogenous. Prior to freeze-drying, final degassing was carried out in a vacuum chamber (50 mTorr) and 15.6 ml of the suspension was pipetted into a stainless-steel tray (internal diameter 60 mm × 60 mm) and freeze-dried at a constant cooling rate of 1 °C/min to a final freezing temperature of −10 °C and dried under a vacuum pressure of 200 mTorr. Cylindrical scaffold plugs 7 mm in diameter were then cut using a biopsy punch.

In order to achieve the required mechanical and degradation properties to support chondrogenesis, the cartilage layer scaffold combined type II collagen, the main collagen component of native cartilage tissue, with type I collagen. This cartilage layer scaffold, consisting of Col1 [0.25% (w/v)], type II collagen (Col2) [0.25% (w/v) porcine Col2, Symatese, France] and hyaluronic acid (HyA) [hyaluronic acid sodium salt derived from streptococcus equi., Contipro, Czech Republic] [0.05% (w/v] [4], was fabricated by adding 0.6 g of Col1 collagen and 0.6 g of Col2 to 200 ml of 0.5 M acetic acid solution. This was blended using an overhead blender (Ultra Turrax T18 overhead blender, IKA Works Inc., USA) at 15,000 rpm at 4 °C for 90 min with repeated visual inspection for clumping and to ensure all collagen was homogenously distributed throughout. 0.11 g of HyA was solubilised in 40 ml of 0.5 M acetic acid and then added dropwise to the blending type I/type II collagen suspension. The blender was maintained at 15,000 rpm for a further 90 min. Prior to freeze-drying, degassing was carried out in a vacuum chamber (50 mTorr) and 15.6 ml of the suspension was pipetted into a stainless-steel tray and freeze-dried at a constant cooling rate of 1 °C/min to a final freezing temperature of −10 °C and dried under a vacuum pressure of 200 mTorr. Cylindrical scaffold plugs 7 mm in diameter were cut from the scaffold sheet using a biopsy punch.

Following this, tri-layered scaffolds were fabricated as previously described [4]. Briefly, the first step involved the fabrication of the bone scaffold as above. Following freeze-drying the scaffold was cross-linked using 1-ethyl-3-(3-dimethylaminopropyl) carbodiimide (EDAC)/N-hydroxysuccinimide (NHS) (Sigma–Aldrich, Arklow, Ireland) at a concentration of 6 mM EDAC/g of collagen, and a 5:2 M ratio of EDAC:NHS for 2 h at room temperature [41]. The scaffold was then hydrated with 0.025 M acetic acid solution in a stainless-steel tray to provide support for the bone layer scaffold during the addition of the next layer. The second step was to add 7.8 ml of the intermediate layer suspension on top of the hydrated bone layer scaffold with freeze-drying repeated as before. The last step involved adding 15.6 ml of the cartilage layer suspension. The process of freeze-drying was repeated as described previously, incorporating prolonged freezing and drying steps to ensure optimal freeze-drying of the tri-layered construct. Following freeze-drying, the scaffolds were dehydrothermally (DHT) cross-linked in a vacuum oven (VacuCell, MMM, Germany) for 24 h. The DHT cross-linking was carried out at a pressure of 50 mTorr, and a temperature of 105 °C to generate cross-links through a condensation reaction, while also sterilising the scaffolds. The entire construct was then chemically cross-linked again under sterile conditions with EDAC as before and dried in the freeze-dryer. Finally, cylindrical scaffold plugs 9.5 mm in diameter were cut from the tri-layered scaffold sheet using a biopsy punch.

2.2. Assessment of the intrinsic ability of the tri-layered scaffold to promote MSC differentiation

2.2.1. BMMSC isolation and cell seeding

The intrinsic ability of the individual layers of the tri-layered scaffold to promote osteogenesis and chondrogenesis was firstly investigated using rat BMMSCs (rBMMSCs). rBMMSCs were isolated from 8-week-old female Fischer 344 rats with the approval of the Research Ethics Committee of the RCSI (REC Approval No. 237). After euthanasia, marrow was flushed from the tibiae and femora with phosphate buffered saline (PBS; Sigma-Aldrich, Ireland) and a single cell suspension was recovered. After centrifugation (600 g, 10 min), cells were plated at 120×10^6 cells/cm^2, in standard rBMMSC growth medium [10% foetal bovine serum (FBS; Hyclone, Fisher Scientific, Ireland), 45% F12-Ham and 45% α-MEM

(Biosciences, Ireland) supplemented with antibiotics (100U/ml penicillin G and 100 μg/ml streptomycin sulphate; Gibco)]. Flasks were incubated at 37 °C in 5% CO_2/90% humidity. After 8 days, colonies became compact and cells were detached with 0.25% trypsin/EDTA and re-plated at 2000 cells/cm^2. Subsequently, cultures were passaged at 5–7 day intervals and expanded to passage 5 for experimentation. The rBMMSCs were cultured in Dulbecco's Modified Eagles Medium 5671 (Sigma-Aldrich, Ireland) supplemented with 2% penicillin/streptomycin (Sigma-Aldrich, Ireland), 1% L-glutamine (Sigma-Aldrich, Ireland), 10% FBS (BioSera, UK), 1% glutamax (Biosciences, Ireland) and 1% non-essential amino acids (Biosciences, Ireland).

The bone layer, intermediate layer and cartilage layer scaffolds were hydrated in PBS until saturated, then placed into non-adherent 24 well plate. rBMMSCs were suspended at a density 1×10^6 cells/34 μl and 17 μl of the cell suspension was then placed on the surface of each scaffold. Scaffolds were incubated at 37 °C for 15 min to allow the cells to attach prior to turning and seeding the other side with a further 17 μl of cell suspension. Scaffolds were incubated at 37 °C for 15 min prior to the addition of 2 ml of complete MSC growth medium to each well of the 24 well plate. The plates were then returned to the incubator at 37 °C in 5% CO_2/90% humidity. MSC growth medium was replaced every 2 days for a period of seven days to allow the cells to attach to and infiltrate into the scaffold.

In order to explore the intrinsic ability of each scaffold to direct MSC differentiation, theywere then transferred to either standard growth medium, osteogenic medium [(Sigma; Dulbecco Modified Eagles Medium 5671, 10% FBS (Biosera; S1900/500), 100 nM Dexamethasone (Sigma; CAS No. 50-02-2), 50 μM Ascorbic acid 2-Phosphate, (Sigma; CAS No. 66170-10-3), 10 mM β-glycerophosphate (Sigma; CAS No. 13408-09-8), 10000 U/mL penicillin and 10 mg/ml streptomycin (Sigma; P4333-100 ml)] or chondrogenic medium [(Dulbecco Modified Eagles Medium D5671), 10% FBS, 2% 10000 U/mL penicillin and 10 mg/ml streptomycin, 0.5% L-Glutamine (Gibco), 0.5% Glutamax 100x (Gibco), 1% non-essential amino acids (NEAA) (Gibco), 20 ng/ml Human TGF-β3 (Prospec), 50 μg/ml Ascorbic Acid, 40 μg/ml Proline (Sigma), 100 nM Dexamethasone (Sigma), 1x ITS supplement (Insulin, transferrin, sodium selenite) (BD), 0.11 mg/ml Sodium Pyruvate (Sigma)]. This timepoint was labelled as day zero.

The bone layer scaffolds were cultured in either standard growth medium or osteogenic growth medium (n = 5 per timepoint). The intermediate layer scaffolds were cultured in osteogenic medium or standard medium (n = 5 per timepoint). The cartilage layer scaffolds were cultured in standard medium or chondrogenic medium (n = 5 per timepoint). One scaffold from each group was prepared for histological analysis. Four scaffolds from each group were flash frozen using liquid nitrogen and stored at −80 °C prior to analysis.

Following assessment of the individual layers, the ability of the tri-layered scaffold as a whole to direct osteogenic and chondrogenic differentiation was investigated. rBMMSCs were seeded onto the tri-layered scaffolds at a seeding density of 0.5×10^6 cells per scaffold using the seeding technique outlined above. Scaffolds were cultured in standard growth medium for one week. The medium was then completely removed and replaced with either standard, chondrogenic, osteogenic or osteochondrogenic medium [(Dulbecco Modified Eagles Medium D5671), 10% FBS, 2% 10000 U/mL penicillin and 10 mg/ml streptomycin, 0.5% L-Glutamine, 0.5% Glutamax 100x, 1% non-essential amino acids (NEAA), 20 ng/ml Human TGF-β3, 50 μg/ml Ascorbic Acid, 40 μg/ml Proline, 100 nM Dexamethasone, 1x ITS supplement, 0.11 mg/ml Sodium Pyruvate, 10 mM β glycerophosphate (Sigma)]. This was marked as Day 0 and the constructs were cultured to timepoints of 14 and 28 days (n = 4) with a partial medium exchange of appropriate supplemented medium every 2–3 days.

2.2.2. Assessment of calcium production

A quantitative calcium assay was performed to assess mineral production in the bone layer and intermediate layer scaffolds cultured in standard and osteogenic medium and to assess calcium production in the tri-layered scaffold when cultured in standard, osteogenic, chondrogenic and osteochondrogenic medium. This assay was performed using a StanBio Calcium Liquicolour Kit (StanBio 0150). Scaffolds were placed on a shaker in 0.5 M HCl over 24–48 h at 4 °C until digested. The assay was then carried out according to the manufacturer's instructions. Briefly, triplicates of 10 μl of each sample were added to 200 μl of working solution (1:1 binding reagent and working dye) in a 96 well plate and absorbance was measured using a photometric plate reader (Wallac 1420 Victor 2 D, Perkin Elmer, MA, USA) based on absorbance at 595 nm against a standard curve of known values.

2.2.3. Assessment of sulphated GAG production

A Blyscan sulphated glycosaminoglycan (sGAG) assay (Biocolour Ltd, UK) was used to measure the quantity of sGAG laid down in the cartilage layer and the intermediate layer scaffolds and to assess calcium production in the tri-layered scaffold when cultured in standard, osteogenic, chondrogenic and osteochondrogenic medium. Samples were digested in papain enzyme solution (10 mg of papain with 10 ml of papain buffer made of PBS, 1% 0.5 M EDTA and 0.79 mg/ml of cysteine-HCl) and 100 μl of each sample was added to 500 μl of Blyscan dye reagent. Tubes were then placed in a mechanical shaker for 30 min to allow the sulphated glycosaminoglycan-dye complex to form and precipitate out of the soluble unbound dye and then spun at 12,000 rpm for 10 min. The Blyscan dissociation agent was then added (500 μl per tube) to release the bound dye back into solution, duplicates of 200 μl of each sample were placed in individual wells of a 96 well plate. Absorbance was measured using a photometric plate reader (Wallac 1420 Victor 2 D, Perkin Elmer, MA, USA) at an absorbance of 656 nm and volumes were determined using a standard curve.

2.2.4. Histological analysis

At each timepoint, one scaffold from each group was fixed in 10% formalin for 1 h for histological analysis and then processed in an automatic tissue processor (ASP300, Leica, Wetzlar, Germany). Scaffolds were then embedded in paraffin wax and sectioned at a thickness of 10 μm using a rotary microtome (RM2255, Leica microtome, Leica). The individual scaffolds were sectioned transversely and tri-layered scaffolds were sectioned longitudinally to demonstrate all layers within a single slice. Sections were stained with Alizarin Red to stain for calcium [42], Toluidine Blue to stain glycosaminoglycans [8], or stained using immunohistochemical staining techniques to identify the presence of type II collagen [33], an important marker of hyaline cartilage formation. Digital images were obtained using a microscope (Nikon 90i, Nikon, Japan) and attached camera unit (Nikon DS Camera control unit, Nikon, Japan) to evaluate the calcium deposition and cartilage production within the individual layers of the scaffold.

2.3. Development of an optimal cell seeding approach for the tri-layered scaffold

2.3.1. CCs, FPMSC and BMMSC isolation

Following assessment of the intrinsic chondrogenic and osteoinductive properties of the tri-layered scaffold using rBMMSCs, a more translationally relevant cell source was then used in order to develop the optimal cell seeding approach for the tri-layered scaffold. Goats are a favourable large animal model for assessment of osteochondral defect repair [43] and our ultimate focus was to test the solution devised in this paper *in vivo* in a caprine model [9] thus the use of goat CCs, BMMSCs

and FPMSCs was explored here. Euthanasia of a skeletally mature male goat was performed, and chondrocytes, FPMSCs and BMMSCs were harvested under Ethics licence approved by the Animal Research Ethics Subcommittee (AREC-P-12-71-Brama). The stifle joint was carefully opened under sterile conditions, and the infrapatellar fat pad was removed in its entirety, placed in PBS and stored at 4 °C. The knee joint was then disarticulated and the cartilage surface exposed. The cartilage was harvested from the distal femur with a 6 mm punch biopsy and the cartilage strips placed in PBS with antibiotic supplementation (100 U/ml penicillin G and 100 μg/ml streptomycin sulphate, and 50 μl of Amphotericin B; Gibco). The distal femur was then opened and the bone marrow was removed using a sterile spatula and placed directly into a 50 ml falcon tube, 5 ml/tube with 10 ml of expansion medium [Gibco DMEM + GlutaMAX (61965, Gibco) + 10% FBS (Foetal Bovine Serum, (Labtech, UK) + 10 ml (100 U/ml penicillin G and 100 μg/ml streptomycin sulphate; Sigma)].

The chondrocytes were isolated from the harvested cartilage tissue using a rapid-isolation technique using collagenase and plastic adherence [25,33,44,45]. The cartilage pieces were removed from the antibiotic supplemented PBS and the cartilage was then sliced to pieces less than 1 mm in size, prior to rinsing again with antibiotic supplemented PBS and placing in sterile 50 ml tubes. Collagenase (Worthington, LS004176 Collagenase Type CLS-2) was dissolved in medium [Gibco DMEM + GlutaMAX (61965, Gibco)] (350 U/ml) (8 ml/g cartilage), and sterile filtered and rotated in the collagenase solution (2 h, 37 °C) prior to passing through a 40 μm cell strainer. Collected cartilage particles were then crushed using a pipette tip and added to 8 ml/g collagenase solution rotating for a further 1 h (37 °C). The sieved medium was added to stopping medium [Gibco DMEM + GlutaMAX (61965, Gibco) + 10% FBS (Foetal Bovine Serum, (Labtech, UK))] of equal volume and mixed. The crushed cartilage was then removed from the rotator and stopping medium of equal volume added and mixed. This was again strained in a 40 μm cell strainer and centrifuged at 650 g for 10 min. The supernatant was discarded, and the pellet re-suspended in standard expansion medium [Gibco DMEM + GlutaMAX (61965, Gibco) + 10% FBS (Foetal Bovine Serum, (Labtech, UK) + 10 ml (100 U/ml penicillin G and 100 μg/ml streptomycin sulphate)] and counted using a trypan blue exclusion test. The chondrocytes were then plated into T175 flasks at a density of 875 × 10^3 cells/flask and expanded to 90% confluency.

The FPMSCs were isolated as per previously published protocols [25,33,44]. The fat pad digestion was carried out using collagenase dissolved in medium (750 U/ml, 4 ml/g of tissue). As previously, the tissue was minced and placed into sterile 50 ml falcon tubes. 4 ml of collagenase solution was added per gram of tissue. The tubes were rotated in a tube rotator at 37 °C for 3–4 h. Two volumes of stopping medium were added to the tissue collagenase mixture. The solution was then passed through a sieve (150 μm) into fresh sterile tubes and centrifuged for 10 min at 650 g. The floating fat fraction containing the adipocytes was aspirated off and discarded. The pellet was resuspended in fresh standard expansion medium and then passed through a 40 μm strainer into a fresh tube. Further medium was added, and the suspension centrifuged once more at 650 g for 5 min. The pellet was resuspended and counted using trypan blue.

The BMMSCs were isolated as previously described [44]. Briefly, the medium/marrow solution was titrated with a 16 G needle to break up any clumps, then the volume was made up to 40 ml using expansion medium and mixed to form a homogenous solution. The tube was then centrifuged twice at 650 g for 5 min, with the supernatant removed and discarded each time. The cell pellet was then resuspended in 10 ml and triturated using a 16 G needle prior to passing through a 40 μm strainer into a fresh and topping up to 20 ml. In order to separate the mononuclear cells, 20 ml of Lymphoprep™ (Axis-Shield, Norway) was placed in a 50 ml falcon tube and the 20 ml suspension added gently on top. The solution then underwent centrifugation for 20 min at 650 g with deceleration set to 0 and acceleration set to 1. When the centrifugation was complete the mononuclear cell layer residing at the interface of the Lymphoprep™ and the cell suspension was removed and cells were counted using trypan blue.

The ability of the isolated FPMSCs and BMMSCs to differentiate down osteogenic, chondrogenic and adipogenic routes was then assessed to confirm their tripotentiality. To assess osteogenic potential, cells were cultured at a density of 1 × 10^5 cell per well in 6 well plates (n = 6) in osteogenic media [10% foetal bovine serum (FBS; Hyclone, Fisher Scientific, Ireland), 90% DMEM + GlutaMAX (Gibco) supplemented with antibiotics (100 U/ml penicillin G and 100 μg/ml streptomycin sulphate; Gibco) dexamethasone 0.4 μg/ml (Sigma), β-glycerol phosphate 0.01 M (Sigma) and ascorbic acid 6.9 mg/ml (Sigma)] opposite negative controls in standard expansion media for a total of 21 days followed by staining with alizarin red (Sigma) staining for calcium. To assess chondrogenisis cell pellets with 250,000 cells per pellet were cultured in a chondrogenic media [10% foetal bovine serum (FBS; Hyclone, Fisher Scientific, Ireland), 90% DMEM + GlutaMAX (Gibco) supplemented with antibiotics (100 U/ml penicillin G and 100 μg/ml streptomycin sulphate; Gibco) with 10 ng/ml of TGF-β3 (R&D Systems) Dexamethasone 0.4 μg/ml (Sigma), ascorbic acid 0.5 mg/ml (Sigma), lineloic acid 47 μg/ml (Sigma), and ITS 1X; (Sigma)] for 7 days and assessed for sulphated GAG levels using Blyscan Sulphated Glycosaminoglycan (sGAG) assay (Biocolour Ltd, UK). Lastly, to assess adipogenic ability cells were seeded at a density of 1 × 10^5 cell per well in 6 well plates (n = 6) and then cultured in adipogenic media [10% foetal bovine serum (FBS; Hyclone, Fisher Scientific, Ireland), 90% DMEM + GlutaMAX (Gibco) supplemented with antibiotics (100 U/ml penicillin G and 100 μg/ml streptomycin sulphate; Gibco) dexamethasone 20 μg/ml, (Sigma) 0.5 mM IBMX (Sigma) 50 μM indomethacin (Sigma)] opposite negative controls in standard expansion media for 21 days. The presence of vacuoles observed using optical microscopy indicated adipogenesis of the MSCs. Cell viability was assessed using trypan blue exclusion.

2.3.2. Identification of optimal cell seeding approach

The harvesting of BMMSCs in a clinical setting presents significant challenges that reduce their potential for use in a single-stage surgical approach. The harvesting procedure would require either lengthening the wound and performing a tibial osteotomy to harvest cells [12], or creating a second surgical site at a different location, i.e. the iliac crest, which would increase surgery time as well as the impact on the patient. Due to these limitations, an initial comparison of the chondrogenic potential of goat BMMSCs and FPMSCs was firstly carried out. BMMSC and FPMSC cell pellets containing 250,000 cells were firstly created by centrifugation and the cells were cultured in pellet form in a chondrogenic medium (n = 3). The pellets were cultured with a medium change every 2–3 days, and three samples of each were taken off at day 0 and day 7. These samples were then assessed for sGAG production using the Blyscan sGAG assay as above. This comparison showed that higher levels of chondrogenesis were achieved from the FPMSCs than the BMMSCs (Supplementary Figure S1). Therefore, BMMSCs were not taken forward to the next stage of testing.

To compare chondrogenesis between the cell types, the cartilage layer of the tri-layered scaffold was utilised. Scaffolds were seeded with CCs and FPMSCs according to the following five groups (Fig. 1). CCs were seeded at a low seeding density (CC LD) of 125,000 cells per scaffold, and a high-density (CC HD) at 500,000 cells per scaffold. The low-density group (CC LD) was selected to mimic a clinical situation by providing a relevant number of chondrocytes to that available clinically from a subcritical size defect, likely to self-heal. The high-density group (CC HD) was designed to mimic the use of expanded cells as currently used in ACI and MACI procedures. FPMSCs were also seeded on the scaffold at a low seeding density of 125,000 (FPMSCs LD) and a high seeding density of 500,000 (FPMSCs HD). The final group consisted of a co-culture of

FPMSCs and CCs at a ratio of 3:1 of FPMSC to CCs and a seeding density of 500,000 cells per scaffold (FPMSCs:CC). This group reflects the number of CCs that can be harvested from a subcritical defect without expansion (125,000, i.e. the CC LD group), augmented with FPMSCs [23,35].

Following cell seeding, scaffolds were cultured in standard growth medium for 3 days to facilitate cell attachment and infiltration into the scaffold. Scaffolds were then cultured in chondrogenic medium for 0, 14, 21 and 28 days. At each timepoint, four scaffolds from each group were flash frozen in liquid nitrogen and stored at −80 °C prior to sGAG was quantified as described above. At each timepoint, one scaffold from each group was prepared for histological analysis as described above. Sections were stained with haematoxylin & eosin staining (H&E) to assess cell proliferation and infiltration, (haematoxylin stains the DNA and RNA rich cell nuclei purple, eosin stains the extracellular matrix pink). Sections were also stained with safranin-O to evaluate cartilage production (safranin-O stains sGAG red). Digital images were captured as before.

2.4. Statistical analysis

All statistical analyses were performed using statistics software Prism 7 GraphPad (GraphPad Software, California USA). Statistical significance was assessed using One-way analysis of variance (ANOVA) or Two-way ANOVA followed by a pairwise multiple comparison procedure (Tukey test). Statistical significance was declared at $p \leq 0.05$.

3. Results

3.1. Assessment of osteogenesis within the bone layer scaffold

Osteogenic differentiation of rBMMSCs in the bone layer scaffold (0.5% (w/v) Col1, 1% (w/v) HA) in osteogenic medium was demonstrated by quantification of calcium deposition within the scaffold. A significant increase in the amount of calcium laid down by rBMMSCs in the bone layer of the scaffold was observed over the 28-day duration of the study when cultured in osteogenic medium ($p < 0.001$) (Fig. 2A), with a 2.48-fold increase in the mineralisation in the scaffold between day 0 and day 28. This demonstrates the ability of the scaffold to support osteogenic differentiation of the scaffold and thus its osteoconductive properties. Having demonstrated the ability of the bone layer scaffold to support the osteogenic differentiation of rBMMSCs in osteogenic medium, the osteoinductive properties were then assessed by culturing the seeded scaffolds in standard growth medium. Calcium levels were seen to have a 1.74-fold increase between day 0 and day 28 ($p < 0.001$) indicating that mineral is being deposited by the rBMMSCs within the scaffold, without the addition of any exogenous osteogenic factors (Fig. 2B). This demonstrates the potential osteoinductive properties of the scaffold resulting from its composition, microarchitecture and mechanical properties. This supports the findings of a previous study that demonstrated the osteoinductive properties of this bone layer scaffold by showing its capacity to form ectopic bone after surgical implantation into the rat hind limb muscle pouch model [46]. Histological analysis of the scaffolds at each timepoint supported the results of calcium quantification (Fig. 2C). Alizarin red staining was positive at all timepoints as a result of the presence of HA within the scaffold composition. HA was observed to be evenly distributed throughout the scaffold microarchitecture at Day 0. The intensity of staining was observed to increase over the 28-day time frame with mineral deposition observed throughout the scaffold. At the 21 and 28 day timepoints in both groups, higher levels of staining were observed in the osteogenic media group than the standard media group, with the highest intensity staining observed towards the periphery of the scaffold indicating potentially higher cell density in this region.

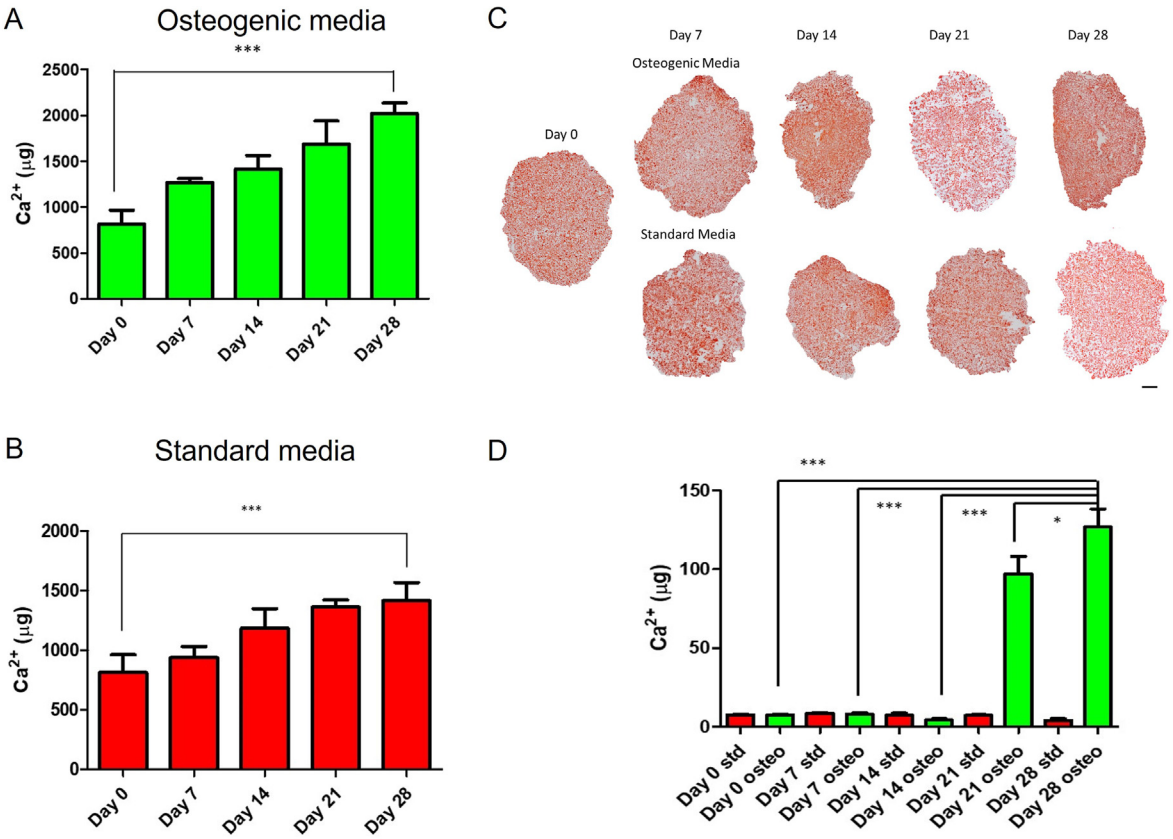

Fig. 2. Calcium deposition in the bone layer scaffold and intermediate layer scaffold. A) Calcium deposition in the bone layer scaffold in osteogenic media. B) Calcium deposition in the bone layer scaffold in standard growth media. C) Alizarin red staining of the bone layer scaffold in osteogenic and standard media (Scale = 1000 μm). D) Calcium deposition in intermediate layer scaffold. (***$p \leq 0.001$, *$p \leq 0.05$).

3.2. Assessment of osteogenesis within the intermediate layer

Mineral deposition in MSC seeded intermediate layer scaffolds (0.5% (w/v) Col1, 0.05% (w/v) HyA) in standard medium and osteogenic medium at timepoints up to 28 days showed an increase in the calcium deposition in the osteogenic medium group over the 28-day culture period, whereas there were no significant levels of calcium observed in the standard growth medium group (Fig. 2D). This demonstrates that while the intermediate layer scaffold can support osteogenesis in osteogenic supplemented medium, it does not have intrinsic osteoinductive properties.

3.3. Assessment of chondrogenesis in the cartilage layer scaffold

Following the assessment of osteogenesis within the bone layer and intermediate layer scaffolds, the chondrogenic properties of the cartilage layer scaffold (0.25% (w/v) Col1, 0.25% (w/v) Col2, 0.05% (w/v] HyA) were then examined using a sGAG assay. Culture of rBMMSCs within the cartilage layer scaffold in chondrogenic medium containing TGF-β3 showed significant increases in sGAG deposition at each timepoint with a 10-fold increase ($p < 0.0001$) in sGAG production over the 28 day study (Fig. 3A). This demonstrates the ability of the scaffold to support rBMMSC chondrogenesis. Culture of this scaffold with rBMMSCs in standard growth medium demonstrated a significant increase in chondrogenesis at day 14 compared to day 0 ($p = 0.0274$) and day 7 (0.0269), demonstrating the ability of the scaffold to direct stem cells toward a chondrogenic lineage without exogenous stimulus. There was, however, no significant difference between the 21 and 28 timepoints (Fig. 3B). Toluidine blue for sGAG deposition (Fig. 3C) and staining for type II collagen (Fig. 3D) showed positive staining at all timepoints due to the presence of both sGAG and type II collagen in the scaffold composition. An increase in the amount of sGAG and collagen II staining in the cartilage layer scaffolds cultured in both medium types was observed over time, with higher levels in the chondrogenic media group as expected.

3.4. Assessment of osteogenesis and chondrogenesis within the tri-layered scaffold

Having demonstrated the osteoinductive properties of the bone layer and chondrogenic properties of the cartilage layer, this study aimed to assess the differentiation of BMMSC in the complete tri-layered scaffold. While separate osteogenic and chondrogenic culture of BMMSCs has been well established within the literature [47], the *in vitro* culture of osteochondral scaffolds containing both a cartilage layer and a bone layer has presented a challenge. Thus, we explored osteogenesis and chondrogenesis in the tri-layered scaffolds cultured in standard growth medium, osteogenic, chondrogenic and osteochondrogenic medium at timepoints of 0, 14, 21 and 28 days. Assessment of osteogenesis in the tri-layered scaffold in osteogenic media showed a significant increase in calcium production at day 28 compared to standard, chondrogenic and osteochondrogenic media types at day 28 and to all groups at day 14, 21 and 28 (Fig. 4A). In order to qualify the results generated, and to assess the distribution of deposited mineral, histological analysis of the tri-layered scaffold was carried out. Alizarin red staining demonstrated that in all media types, calcium deposition was confined to the bone and intermediate layers of the scaffold with greater levels of staining in the bone layer. As expected, greater levels of staining were observed in the osteogenic media than in the other media types. Mineral was seen to be evenly distributed throughout the bone layer. No positive mineral staining was observed in the cartilage layer (Fig. 4B). sGAG quantification also demonstrated an increase in sGAG content over time, with significantly higher levels of sGAG production in both the chondrogenic medium ($p = 0.0106$) and the osteochondrogenic medium ($p = 0.0233$)

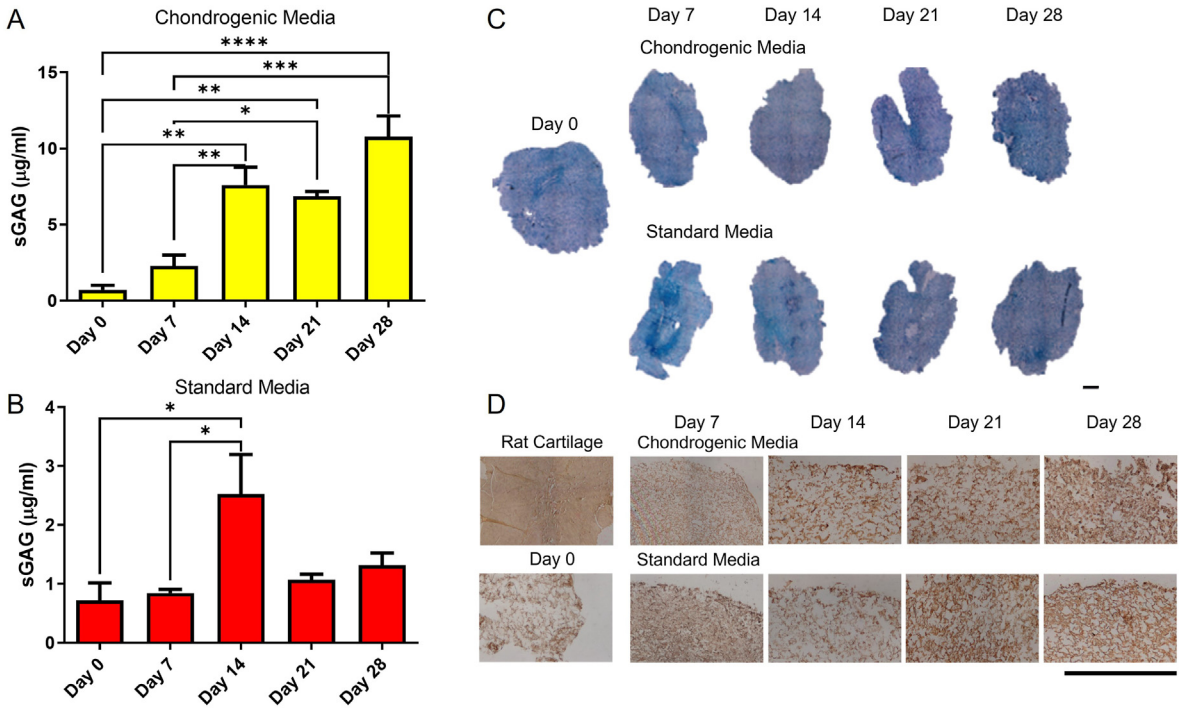

Fig. 3. Chondrogenesis in the cartilage layer scaffold. A) Quantification of sGAG in the cartilage layer in chondrogenic media. B) Quantification of sGAG in the cartilage layer in standard growth media. C) Toluidine Blue staining of cartilage layer scaffold cultured in chondrogenic media and standard media (Scale = 1000 μm). D) Collagen II immunohistochemical staining of cartilage layer scaffold (Scale = 500 μm). (****$p \leq 0.0001$, ***$p \leq 0.001$, **$p \leq 0.01$, *$p \leq 0.05$).

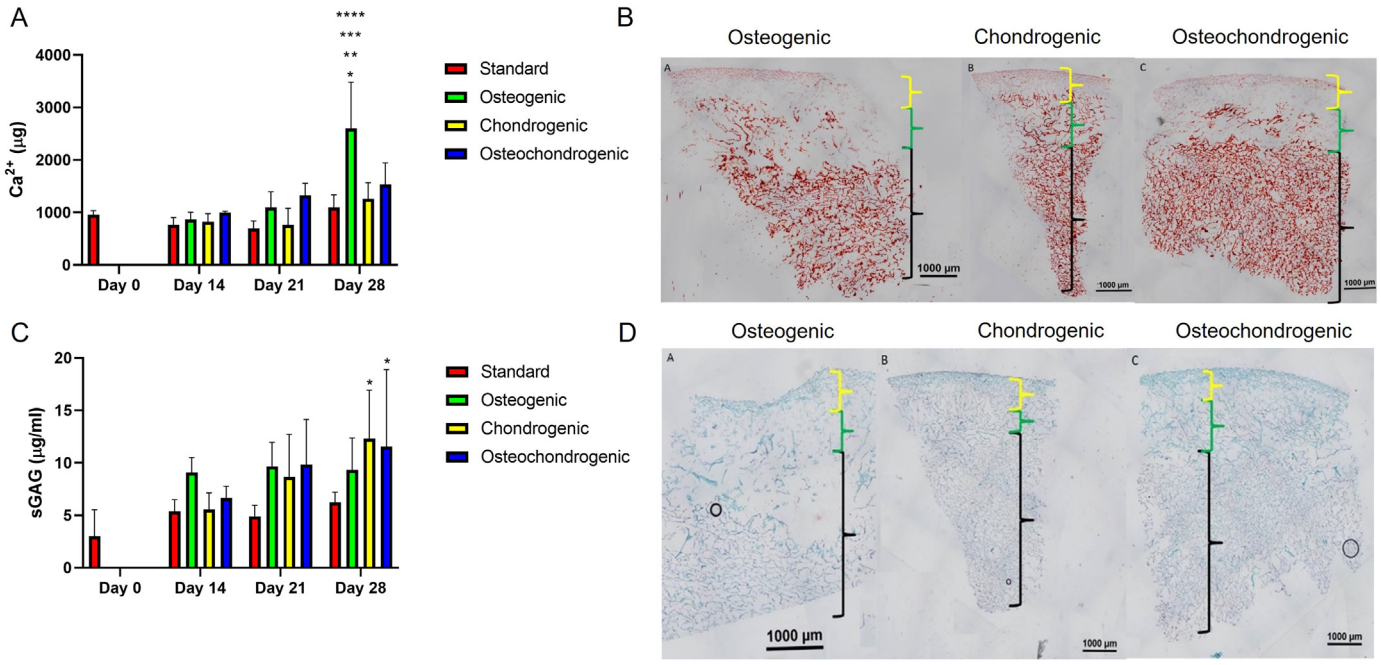

Fig. 4. Chondrogenesis and osteogenesis in the tri-layered scaffold. A) Calcium deposition in the tri-layered scaffold in standard, osteogenic, chondrogenic and osteochondrogenic media. B) Alizarin Red staining for calcium at day 28 following culture in osteogenic media, chondrogenic media, osteochondrogenic media (Black = bone layer, green = intermediate layer, yellow = cartilage layer) C) sGAG deposition in the tri-layered scaffold over 28 days in standard, osteogenic, chondrogenic and osteochondrogenic media. D) Toluidine Blue staining of representative samples of the scaffolds at day 28 cultured in standard, osteogenic, chondrogenic and osteochondrogenic media (Black = bone layer, green = intermediate layer, yellow = cartilage layer).

at day 28 compared to day 0 (Fig. 4C). Toluidine blue staining of the tri-layered scaffold confirmed cartilage matrix formation predominantly within the cartilage layer (Fig. 4D). No difference in the intensity or distribution of staining could be observed between the three media types.

3.5. Development of optimal cell seeding approach

The optimal cell culture regime and cell seeding density were then investigated by quantifying sGAG deposition within the cartilage layer scaffold cultured with the different regimes. At day 0 highest levels of sGAG deposition were observed in the high density chondrocyte (CC HD) group compared to all other groups (Fig. 5A). Higher sGAG deposition was also observed in the low density chondrocyte (CC LD) group compared to the low density FPMSC (FPMSCs LD) group ($p = 0.0024$). For the day 14 (Fig. 5B) and day 21 (Fig. 5C) timepoints significantly higher levels of sGAG deposition was observed in the FPMSCs:CC co-culture group compared to all other groups. At day 28 the highest level of sGAG deposition was again observed in the FPMSCs:CC co-culture group with significantly higher levels observed compared to both the FPMSCs LD ($p = 0.0040$) and CC LD ($p = 0.0040$) groups (Fig. 5D). These results show that the addition of FPMSCs to the CC LD group (i.e., the FPMSC:CC group) led to a 7.8-fold increase in sGAG over the CC LD by day 28. Notably, the levels sGAG produced by FPMSCs and CCs were significantly higher than the sGAG levels deposited by rBMMSCs despite the higher seeding density of 1×10^6 cells per scaffold in the rBMMSCs study (Fig. 3). H&E staining (Fig. 6) showed that cells were concentrated around the periphery of the scaffold at day 14 with increased migration towards the centre of the scaffold observed at the day 21 and day 28 timepoints. In general, lower levels of cell migration were observed in the FP LD and CC LD groups than in FP HD, CC HD and FPMSC:CC groups. Regions of high proliferation were observed at day 28 in the CC HD, FP HD and FPMSCs:CC groups (Fig. 6 Day 28 B, D and E).

Safranin-O staining (Fig. 7) confirmed the findings of the quantitative analysis with increased uptake of red/purple stain demonstrating higher levels of sGAG deposition in the higher seeding density groups. At early timepoints, staining was observed mainly in the periphery of the scaffold with migration of cells and positive staining observed towards the centre of the scaffold at day 21 (Fig. 7-Day 21 E). By day 28, sGAG deposition appeared to be more evenly distributed throughout the scaffolds with visibly higher levels of staining observed for the FP HD, CC HD and FPMSC:CC co-culture groups over the other groups (Fig. 7- Day 28 B, D and E). Taken together these results indicate that the highest levels of chondrogenesis were achieved in the FPMSC:CC group compared to other groups.

4. Discussion

Osteochondral defects are challenging to treat due in part to the heterogeneous gradient nature of osteochondral tissue. While cell-free scaffolds have shown potential for the treatment of focal osteochondral defects, cell-seeded scaffolds may offer enhanced regenerative potential and enable the treatment of larger joint defects. However, current approaches require *in vitro* expansion, with associated limitations relating to costs and increased surgical time. Therefore, the goal of this study was to identify a cell seeding approach that would enable a single-stage surgical approach without the requirement for *in vitro* expansion of cells. Initially, the intrinsic ability of a tri-layered scaffold previously developed in our group to direct stem cell differentiation was explored. The results show that the tri-layered scaffold has the capability to direct the differentiation of bone marrow MSCs (BMMSCs) down an osteogenic

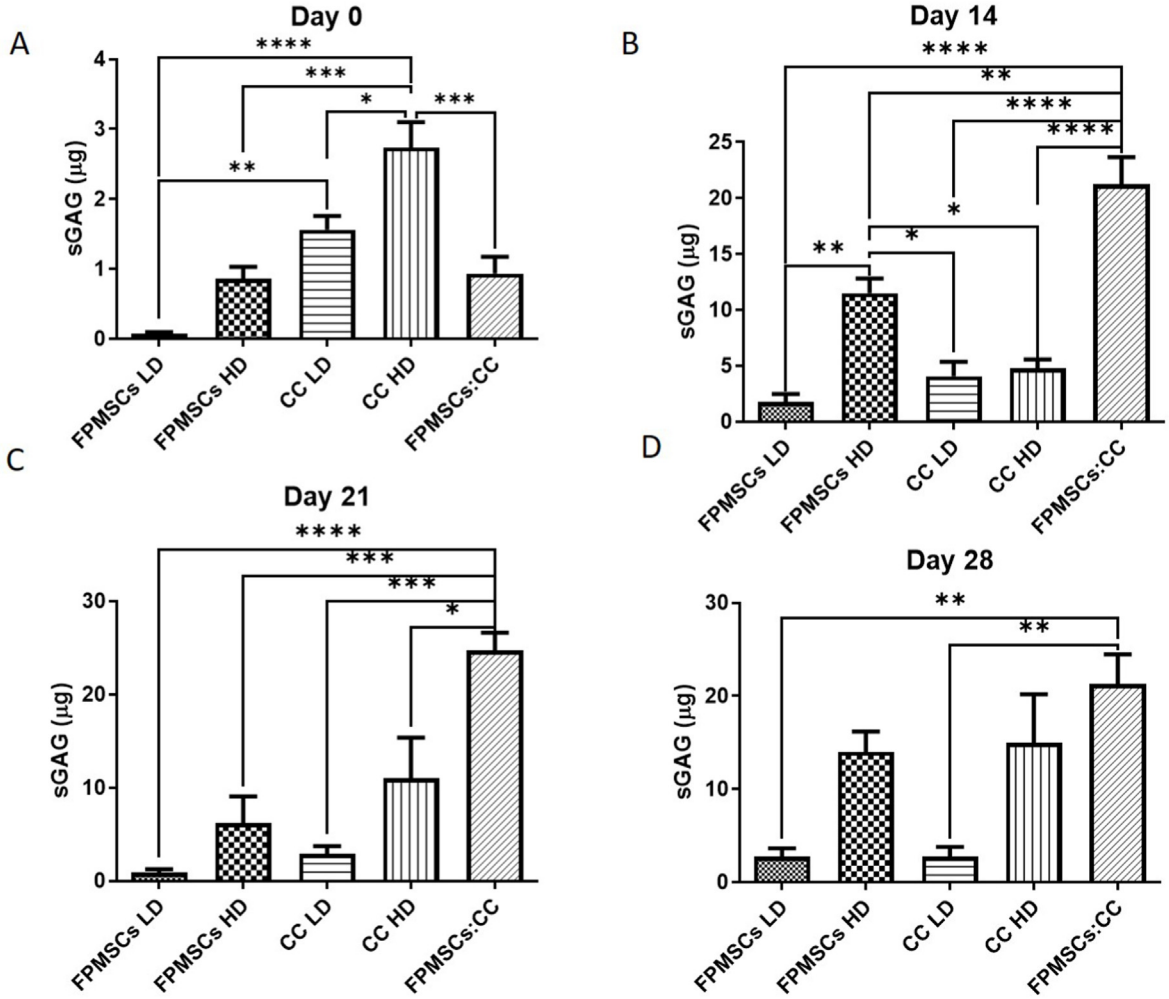

Fig. 5. sGAG deposition in the cartilage layer scaffold seeded with FPMSCs at low and high density (FPMSCs LD and FPMSCs HD). CCs at low and high density (CC LD and CC HD) and a co-culture of FPMSCs and CCs (FPMSCs:CC). A) At day 0 a significant increase in sGAG production was observed in the CC LD group compared to the FMSCs LD group and in the CC HD group compared to other groups. B) At day 14 a significant increase in sGAG in the co-culture group was observed over all groups. C) At day 21 again the co-culture group shows significantly higher levels of sGAG production over all other groups. D) At day 28 significantly higher sGAG levels were observed in the co-culture group compared to the FPMSC LD, and CC LD groups. (****$p \leq 0.0001$, ***$p \leq 0.001$, **$p \leq 0.01$, *$p \leq 0.05$).

route leading to bone formation confined within the bone layer and down a chondrogenic route leading to cartilage formation confined within the uppermost cartilage layer. In order to enhance the regenerative potential of this tri-layered scaffold, chondrogenesis within the cartilage layer of the scaffold following seeding with rapidly isolated CCs and FPMSCs, at low and high seeding densities or as a FPMSC:CC co-culture was then investigated. The results demonstrated that a co-culture of FPMSCs and CCs represented the optimal seeding approach with a 7.8-fold increase in the sGAG production observed in this group compared to seeding with chondrocytes alone (CC LD). This approach demonstrates that by adding FPMSCs to a relatively small number of chondrocytes high levels of chondrogenesis can be achieved while avoiding the requirement for *in vitro* expansion.

The intrinsic properties of the tri-layered scaffold to direct MSC differentiation were explored using bone marrow derived MSCs. The ability of the individual scaffold layers to direct osteogenesis and chondrogenesis was firstly assessed, prior to exploring calcium and sGAG deposition by rBMMSCs within the full tri-layered scaffold. Quantification of mineral deposition within the bone layer of the tri-layered scaffold demonstrated the scaffold's ability to support osteogenesis. The results show a 2.48-fold increase in the mineral deposition within the scaffold between the Day 0 and Day 28 timepoints when cultured in osteogenic medium, demonstrating the osteoconductive properties of the scaffold. These results support the findings of previous studies where the ability of this scaffold to support mineralisation by MC3T3 mouse pre-osteoblast cells was demonstrated [4,42]. Furthermore, the intrinsic properties of the scaffold were also shown to direct the osteogenic differentiation of MSCs without exogenous growth factors indicating the osteoinductive properties of the scaffold [48,49]. The results show a 1.74-fold increase in the mineral deposition in standard growth medium without any exogenous osteogenic growth factors thus demonstrating the scaffold's potential ability to direct the osteogenic differentiation of infiltrating MSCs following implantation of the scaffold into an osteochondral lesion. Cells bind to collagen scaffolds through integrin-mediated cell adhesion. Type I collagen possesses multiple binding sites, such as GFOGER and GROGER, capable of being recognized by α_2 I and α_{10} I domains of integrin respectively [50,51]. The interaction of the α_2 integrin subunit, a component of major collagen receptor $\alpha 2\ \beta\ 1$ integrin, with type 1 collagen plays a crucial role in the expression of osteoblastic phenotypes of MSCs [52,53]. The osteoinductive properties of the scaffold are promoted as a result of the presence of HA particles [42,48,49,54]. The combination of Ca^{2+} and PO_3^{-4} ions trigger osteogenic differentiation through BMPs/SMAD and RAS signalling pathways, involving genes typically regulated during dexamethasone (DEX) induced differentiation

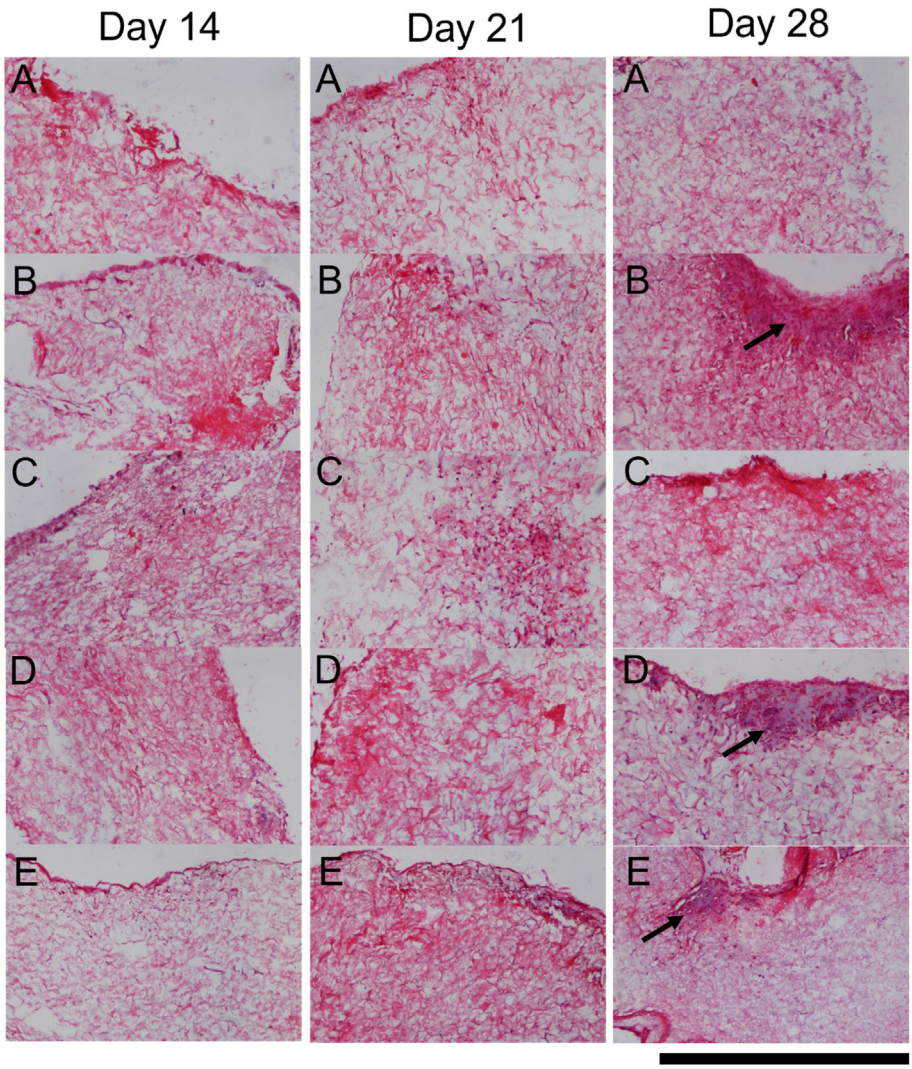

Fig. 6. H&E staining of representative samples from Day 14, 21 and 28 for each cell group. A) Low density FPMSCs (FPMSCs LD) B) High density FPMSCs (FPMSCs HD), C) Low density CCs (CC LD), D) High density CCs (CC HD) and E) Co-culture of FPMSCs and CCs (FPMSCs:CC). Areas of high proliferation are visible in B, D and E at the day 28 timepoint, showing increased cell proliferation in the high seeding density groups (Black arrows). Scale = 500 μm.

[55]. The stiffness of the scaffold has also been shown to influence the differentiation of MSCs [56,57]. Specifically, RUNX2 expression, an indicator of osteogenic differentiation, by MSCs on collagen-based scaffolds of similar stiffness to the bone layer scaffold investigated here (1.5 kPa) has been shown to be higher compared to expression on scaffolds of lower stiffness [56].

The intermediate layer of the scaffold is aimed at regenerating the calcified cartilage layer of the native joint and is a protective tidemark against the vascularisation and encroachment of the subchondral bone into the cartilage layer. Such encroachment can cause thinning of the overlying cartilage and can even exacerbate the initial morbidity. It is often seen following repair techniques, such as microfracture, and in scaffold-free repair [58,59]. Therefore, one of the most important findings relating to the intermediate layer was that a significant increase in mineral deposition in standard growth medium was not demonstrated. Alizarin red staining of the tri-layered scaffold showed no mineralisation advancing beyond the tidemark and into the cartilage layer over the course of the study. It can therefore be surmised that when implanted in the joint and exposed to the stimulating differentiation factors, the intermediate layer will resist mineralisation and protect the overlying cartilage from hypertrophy and vascularisation which would lead to ossification and thinning of the gliding surface [9,60].

Chondrogenesis by MSCs was observed within the cartilage layer scaffold in the presence of chondrogenic factors as demonstrated by an increase in sGAG levels. Chondrogenesis was also observed in standard growth medium without exogenous chondrogenic supplements, albeit to a lesser extent. This indicates that the scaffold has some intrinsic ability to guide differentiation of MSCs down a chondrogenic route. Matrix produced within the scaffold was shown, using immunohistochemistry, to contain collagen type II consistent with hyaline cartilage. Hyaline cartilage repair is preferable to fibrocartilage repair, found with bone marrow stimulating repair techniques, as fibrocartilage is a mechanically inferior scar tissue unable to deal with the shear stresses and strains of the articulation [61–63]. Both type I and II collagen have been shown to support the attachment, proliferation and chondrogenic differentiation of MSCs [64]. The increased collagen type II observed within the cartilage layer scaffold is consistent with the increased sGAG and stimulation of matrix production seen in other scaffolds fabricated using type II collagen [50,65,66]. The chondroinductive properties of type II collagen reportedly derive through β1 integrin-mediated Rho A/Rock signalling [50]. The HyA component of the cartilage layer has also been shown to promote chondrogenesis [67,68]. Cells interact with HyA through surface receptors such as CD44, which enable modulation of cell activities such as migration, proliferation and differentiation, as well as matrix secretion [67,69]. The tailored stiffness of the cartilage layer of the tri-layered scaffold also plays a role in promoting chondrogenesis.

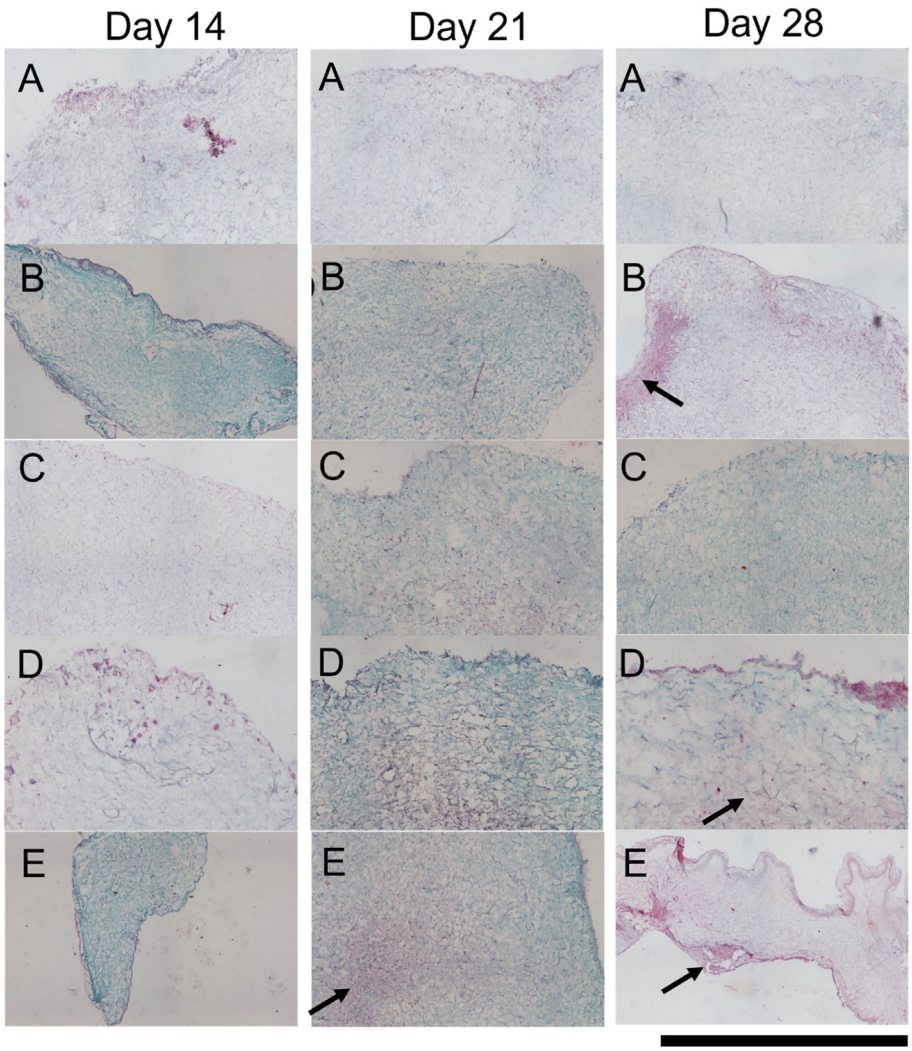

Fig. 7. Safranin-O staining of scaffolds seeded with each cell group at Day 14, Day 21 and Day 28. A) Low density FPMSCs (FPMSCs LD) B) High density FPMSCs (FPMSCs HD), C) Low density CCs (CC LD), D) High density CCs (CC HD) and E) Co-culture of FPMSCs and CCs (FPMSCs:CC). Higher levels of sGAG deposition were observed in the co-culture group (E) at day 21 and the high-density groups (B, D and E) at day 28 (black arrows). Scale = 500 μm.

Scaffolds with stiffnesses in the range of 0.5 kPa–1 kPa have previously been shown to promote SOX9 expression and thus induce MSCs differentiation down a chondrogenic lineage [56].

Investigation of a suitable culture media formulation for *in vitro* culture of osteochondral scaffolds demonstrated that a combination medium containing both chondrogenic and osteogenic supplemented factors, i.e., osteochondrogenic medium, enabled chondrogenic and osteogenic differentiation of BMMSCs within the relevant regions of the tri-layered scaffold. Attempting to recreate an environment *in vitro* to replicate the gradient nature of the osteochondral defect is a challenge that has not been explored greatly in the literature. There have been some attempts at a minimum common differentiate medium [70] mixed medium [71] or using custom wells with a membranes separating the layers of scaffold into different medium types [72]. The results show that the tri-layered scaffold, when cultured as a whole in an osteochondrogenic medium, has the ability to cause an increase in sGAG in the cartilage layer and a simultaneous increase in the mineralisation in the calcium layer while maintaining the tidemark in between. These findings further demonstrate the intrinsic ability of the tri-layered scaffold to promote chondrogenesis and osteogenesis with the requisite layers of the scaffold.

Following demonstration of the intrinsic osteogenic and chondrogenic properties of the tri-layered scaffolds, the study then explored cell seeding techniques with the aim of enhancing the regenerative potential of the scaffold. In order to develop the optimal approach for osteochondral defect repair a rapid isolation approach was successfully used to isolate bone marrow mesenchymal stem cells, fat pad mesenchymal stem cells and chondrocytes. Currently cell-based therapies for cartilage repair require two operations, with a gap of roughly six weeks in order to harvest and expand the chondrocytes *in vitro* prior to re-implantation [12,73]. This means that the patient has to rehabilitate twice, as well as the increased financial costs of the surgery and the *in vitro* expansion [15]. Rapid isolation and immediate re-implantation of cells seeded onto the scaffold using this single-stage approach would overcome the challenges of existing techniques. Here BMMSCs and FPMSCs were explored as potential cell sources. The harvesting BMMSCs has some disadvantages as it requires either lengthening the wound and performing an osteotomy [12], while FPMSCs can be harvested through same arthroscopic incision as the CCs which limits the insult to only one surgical site. Furthermore, an assessment of the chondrogenic potential of these cells shown higher levels of chondrogenesis were achieved by FPMSCs than BMMSCs. Therefore, only MSCs derived from the fat pad were taken forward. A further advantage of FPMSCs is that they have been shown to maintain their chondrogenic capacity in osteoarthritic donors [74], which is crucial in order to be able to treat those who present late with the defect. A further advantage of this cell type is that allogenic FPMSCs have shown potential for therapeutic application which would eliminate the need to

harvest the patient's own cells. Han et al. demonstrated that the allogenic FPMSCs effectively achieved repair of the articular cartilage in a rabbit articular cartilage defect model without eliciting a negative immune response [75]. Furthermore, Toghraie et al. explored the use of allogenic FPMSCs in a rabbit OA model and reported that no obvious immunologic response was observed [76].

When examining the cartilage formation within the cartilage layer scaffold, the high seeding density groups demonstrated increased cartilage formation compared to the low seeding density groups [77–79]. Overall, at both high and low seeding densities CCs resulted in higher sGAG production than FPMSCs, which is consistent with both their phenotype, and previous studies [80]. However, the highest levels of chondrogenesis was observed in the co-culture group, where FPMSCs and CCs were combined in a 3:1 ratio [23,35]. The FPMSC:CC group investigated here uses the same overall number of cells as both the CC HD and the FPMSC HD groups. This important result shows that there is a synergistic effect of the co-culture, whereby the FPMSCs and the CCs together can achieve a higher level of sGAG production than either can separately. It is also important to note that the number of CCs used in the FPMSC:CC group is the same as the clinically relevant number used in the CC LD group. While the exact molecular mechanism leading to the increase in sGAG production in co-cultures of CCs and MSCs over CCs and MSCs monocultures is still unclear, multiple mechanisms have been postulated [34–40,81]. Acharya et al. report that within CC:MSC co-cultures a limited fraction of the MSC population was stimulated to express higher type II collagen and lower type X collagen, and chondrocytes proliferated without losing their differentiated phenotype [81]. However, studies by Wu et al. and Meretoja et al. report that increased chondrogenesis in CC:MSC co-cultures was not due to increased chondrogenic differentiation of MSCs and instead resulted from chondrogenic inducing cytokines and growth factors, e.g. TGF-betas, BMP-2 and IGF-1, produced by MSCs exerting a trophic effect on the chondrocytes, stimulating their proliferation and matrix deposition [39,40]. More recently, Huang et al. reported that CC:FPMSC co-cultures did not change the chondrogenic capacity of either cell type, with no significant difference in expression of the marker genes COL2A1, ACAN, and SOX9 between the CC:FPMSC co-culture group and the monoculture controls. In addition, they report no significant difference in COL1A1 expression between CC monoculture and the co-culture group, indicating that the fibroblastic differentiation of CCs was not reduced in the co-culture. They propose that hypertrophy of MSCs was inhibited in co-culture, with a significant difference in COL10A1 expression between the MSC monoculture group and the co-culture group observed. This inhibition of MSC hypertrophy might be attributed to the parathyroid hormone-related protein (PTHrP) secreted by CCs throughout the coculture as reported by Fischer et al. [38].

This shows that, avoiding the *in vitro* expansion phase by adding FPMSCs to a relatively small number of chondrocytes, can lead to an almost 8-fold increase in the sGAG produced over just the chondrocytes alone further demonstrating the potential of this methodology as a single-stage cell-based approach for osteochondral defect repair.

Taken together, the above findings demonstrate the layer specific osteoinductive and chondrogenic properties of our tri-layered scaffold resulting from the macromolecules present in each layer of the scaffold. These results demonstrate the capability of this biomimetic scaffold to direct the differentiation of infiltrating BMMSCs. Exploring the optimal cell seeding approach showed highest levels of chondrogenesis were obtained when seeding the scaffold with a co-culture of FPMSC:CC, isolated using a rapid isolation technique, due to the synergistic effect of the co-culture. Overall, this study shows the development of a cell-seeded scaffold for osteochondral defect repair based on a single-stage surgical approach that eliminates the requirement for *in vitro* expansion of cells. This approach has the potential to achieve more rapid tissue repair than could be achieved through the use of cell-free scaffolds. The optimal cell group in combination with the tri-layered scaffolds is currently under further investigation in an *in vivo* caprine model. The outcomes of this study will provide important information about the ability of this cell seeding approach to achieve a clinically relevant increase in osteochondral defect repair.

5. Conclusion

This study investigated the optimal cell seeding approach for tri-layered scaffolds designed for osteochondral defect repair. The capability of the intrinsic properties of the tri-layered scaffold to direct stem cell differentiation in each layer of the scaffold was demonstrated. The bone layer demonstrated osteoconductive and osteoinductive properties and the cartilage layer demonstrated chondroconductive properties while the intermediate layer resisted hypertrophy and mineralisation, therefore protecting the tidemark between the subchondral bone and overlying cartilage. The regenerative potential of the scaffold was augmented through the addition of rapidly isolated chondrocytes (CCs) and fat pad MSC cells (FPMSCs). The greatest level of chondrogenesis were achieved in the FPMSC:CC co-culture group, demonstrating a synergistic effect between these two cell types. The results showed that adding FPMSCs to a relatively small number of chondrocytes resulted in a 7.8-fold increase in the sGAG production over chondrocytes alone. We conclude therefore that FPMSC:CC co-culture is a viable method to maximise cartilage production in a single-stage surgical approach. Overall, the combination of the intrinsic properties of the tri-layered scaffold and the optimised seeding approach developed here results in a promising approach for the treatment of challenging osteochondral defects.

Author contributions

Conceptualization – Conor Moran, Tanya J. Levingstone; Data curation – Conor Moran, Tanya J. Levingstone; Formal analysis – Conor Moran, Tanya J. Levingstone; Funding acquisition - Fergal J. O'Brien; Methodology – Conor Moran, Tanya J. Levingstone, Henrique V Almeida; Supervision – Tanya J. Levingstone, Fergal J. O'Brien; Writing – original draft; Conor Moran, Tanya J. Levingstone; Writing – review & editing - Conor Moran, Tanya J. Levingstone, Henrique V Almeida, Daniel J Kelly, Fergal J. O'Brien.

Funding

This work was supported by Science Foundation Ireland (SFI)/ Health Research Board (HRB) Translational Research Award (TRA/2011/19).

Data availability

The raw/processed data required to reproduce these findings cannot be shared at this time due to technical or time limitations.

Declaration of competing interest

The authors declare that they have no known competing financial interests or personal relationships that could have appeared to influence the work reported in this paper.

Appendix A. Supplementary data

Supplementary data to this article can be found online at https://doi.org/10.1016/j.mtbio.2021.100173.

References

[1] R. Andrade, S. Vasta, R. Pereira, H. Pereira, R. Papalia, M. Karahan, J.M. Oliveira, R.L. Reis, J. Espregueira-Mendes, Knee donor-site morbidity after mosaicplasty – a systematic review, J. Exp. Orthop. 3 (2016) 31, https://doi.org/10.1186/s40634-016-0066-0.

[2] E. Solheim, J. Hegna, E. Inderhaug, Long-term survival after microfracture and mosaicplasty for knee articular cartilage repair: a comparative study between two treatments cohorts, Cartilage 11 (2020) 71–76, https://doi.org/10.1177/1947603518783482.

[3] M.T. Frassica, M.A. Grunlan, Perspectives on synthetic materials to guide tissue regeneration for osteochondral defect repair, ACS Biomater. Sci. Eng. 6 (2020) 4324–4336, https://doi.org/10.1021/acsbiomaterials.0c00753.

[4] T.J. Levingstone, A. Matsiko, G.R. Dickson, F.J. O'Brien, J.P. Gleeson, A biomimetic multi-layered collagen-based scaffold for osteochondral repair, Acta Biomater. 10 (2014), https://doi.org/10.1016/j.actbio.2014.01.005.

[5] S. Critchley, E.J. Sheehy, G. Cunniffe, P. Diaz-Payno, S.F. Carroll, O. Jeon, E. Alsberg, P.A.J. Brama, D.J. Kelly, 3D printing of fibre-reinforced cartilaginous templates for the regeneration of osteochondral defects, Acta Biomater. 113 (2020) 130–143, https://doi.org/10.1016/j.actbio.2020.05.040.

[6] S. Ansari, S. Khorshidi, A. Karkhaneh, Engineering of gradient osteochondral tissue: from nature to lab, Acta Biomater. 87 (2019) 41–54, https://doi.org/10.1016/j.actbio.2019.01.071.

[7] I.J.P. Henderson, D.P. La Valette, Subchondral bone overgrowth in the presence of full-thickness cartilage defects in the knee, Knee 12 (2005) 435–440, https://doi.org/10.1016/j.knee.2005.04.003.

[8] T.J. Levingstone, E. Thompson, A. Matsiko, A. Schepens, J.P. Gleeson, F.J. O'brien, Multi-layered collagen-based scaffolds for osteochondral defect repair in rabbits, Acta Biomater. 32 (2016) 149–161, https://doi.org/10.1016/j.actbio.2015.12.034.

[9] T.J. Levingstone, A. Ramesh, R.T. Brady, P.A.J. Brama, C. Kearney, J.P. Gleeson, F.J. O'Brien, Cell-free multi-layered collagen-based scaffolds demonstrate layer specific regeneration of functional osteochondral tissue in caprine joints, Biomaterials 87 (2016) 69–81, https://doi.org/10.1016/j.biomaterials.2016.02.006.

[10] J.D. Stack, T.J. Levingstone, W. Lalor, R. Sanders, C. Kearney, F.J. O'Brien, F. David, Repair of large osteochondritis dissecans lesions using a novel multilayered tissue engineered construct in an equine athlete, J. Tissue Eng. Regen. Med. 11 (2017) 2785–2795, https://doi.org/10.1002/term.2173.

[11] E.B. Hunziker, Articular cartilage repair: are the intrinsic biological constraints undermining this process insuperable? Osteoarthritis Cartilage 7 (1999) 15–28, https://doi.org/10.1053/joca.1998.0159.

[12] M. Brittberg, A. Lindahl, A. Nilsson, C. Ohlsson, O. Isaksson, L. Peterson, Treatment of deep cartilage defects in the knee with autologous chondrocyte transplantation, N. Engl. J. Med. 331 (1994) 889–895, https://doi.org/10.1056/NEJM199410063311401.

[13] T. Shen, Y. Dai, X. Li, S. Xu, Z. Gou, C. Gao, Regeneration of the osteochondral defect by a wollastonite and macroporous fibrin biphasic scaffold, ACS Biomater. Sci. Eng. 4 (2018) 1942–1953, https://doi.org/10.1021/acsbiomaterials.7b00333.

[14] R.L. Dahlin, L.A. Kinard, J. Lam, C.J. Needham, S. Lu, F.K. Kasper, A.G. Mikos, Articular chondrocytes and mesenchymal stem cells seeded on biodegradable scaffolds for the repair of cartilage in a rat osteochondral defect model, Biomaterials 35 (2014) 7460–7469, https://doi.org/10.1016/j.biomaterials.2014.05.055.

[15] E.M. Samuelson, D.E. Brown, Cost-effectiveness analysis of autologous chondrocyte implantation: a comparison of periosteal patch versus type I/III collagen membrane, Am. J. Sports Med. 40 (2012) 1252–1258, https://doi.org/10.1177/0363546512441586.

[16] W. Kafienah, M. Jakob, O. Démarteau, A. Frazer, M.D. Barker, I. Martin, A.P. Hollander, Three-dimensional tissue engineering of hyaline cartilage: comparison of adult nasal and articular chondrocytes, Tissue Eng. 8 (2002) 817–826, https://doi.org/10.1089/10763270260424178.

[17] C. Vinatier, O. Gauthier, A. Fatimi, C. Merceron, M. Masson, A. Moreau, F. Moreau, B. Fellah, P. Weiss, J. Guicheux, An injectable cellulose-based hydrogel for the transfer of autologous nasal chondrocytes in articular cartilage defects, Biotechnol. Bioeng. 102 (2009) 1259–1267, https://doi.org/10.1002/bit.22137.

[18] J.C.H. Leijten, N. Georgi, L. Wu, C.A. Van Blitterswijk, M. Karperien, Cell sources for articular cartilage repair strategies: shifting from monocultures to cocultures, Tissue Eng. B Rev. 19 (2013) 31–40, https://doi.org/10.1089/ten.teb.2012.0273.

[19] W.J.F.M. Jurgens, R.J. Kroeze, B. Zandieh-Doulabi, A. van Dijk, G.A.P. Renders, T.H. Smit, F.J. van Milligen, M.J.P.F. Ritt, M.N. Helder, One-step surgical procedure for the treatment of osteochondral defects with adipose-derived stem cells in a caprine knee defect: a pilot study, Biores. Open Access 2 (2013) 315–325, https://doi.org/10.1089/biores.2013.0024.

[20] W. Ando, K. Tateishi, D.A. Hart, D. Katakai, Y. Tanaka, K. Nakata, J. Hashimoto, H. Fujie, K. Shino, H. Yoshikawa, N. Nakamura, Cartilage repair using an in vitro generated scaffold-free tissue-engineered construct derived from porcine synovial mesenchymal stem cells, Biomaterials 28 (2007) 5462–5470, https://doi.org/10.1016/j.biomaterials.2007.08.030.

[21] W.L. Fu, C.Y. Zhou, J.K. Yu, A new source of mesenchymal stem cells for articular cartilage repair: MSCs derived from mobilized peripheral blood share similar biological characteristics in vitro and chondrogenesis in vivo as MSCs from bone marrow in a rabbit model, Am. J. Sports Med. 42 (2014) 592–601, https://doi.org/10.1177/0363546513512778.

[22] T. Mesallati, C.T. Buckley, D.J. Kelly, Engineering articular cartilage-like grafts by self-assembly of infrapatellar fat pad-derived stem cells, Biotechnol. Bioeng. 11 (2014) 1686–1698, https://doi.org/10.1002/bit.25213.

[23] T. Mesallati, C.T. Buckley, D.J. Kelly, Engineering cartilaginous grafts using chondrocyte-laden hydrogels supported by a superficial layer of stem cells, J. Tissue Eng. Regen. Med. 11 (2017) 1343–1353, https://doi.org/10.1002/term.2033.

[24] C.T. Buckley, T. Vinardell, S.D. Thorpe, M.G. Haugh, E. Jones, D. McGonagle, D.J. Kelly, Functional properties of cartilaginous tissues engineered from infrapatellar fat pad-derived mesenchymal stem cells, J. Biomech. 43 (2010) 920–926, https://doi.org/10.1016/j.jbiomech.2009.11.005.

[25] Y. Liu, C.T. Buckley, H.V. Almeida, K.J. Mulhall, D.J. Kelly, Infrapatellar fat pad-derived stem cells maintain their chondrogenic capacity in disease and can be used to engineer cartilaginous grafts of clinically relevant dimensions, Tissue Eng. 20 (2014) 3050–3062, https://doi.org/10.1089/ten.tea.2014.0035.

[26] Y. Liu, C.T. Buckley, R. Downey, K.J. Mulhall, D.J. Kelly, The role of environmental factors in regulating the development of cartilaginous grafts engineered using osteoarthritic human infrapatellar fat pad-derived stem cells, Tissue Eng. 18 (2012) 1531–1541, https://doi.org/10.1089/ten.tea.2011.0575.

[27] T. Vinardell, E.J. Sheehy, C.T. Buckley, D.J. Kelly, A comparison of the functionality and in vivo phenotypic stability of cartilaginous tissues engineered from different stem cell sources, Tissue Eng. 18 (2012) 1161–1170, https://doi.org/10.1089/ten.tea.2011.0544.

[28] S.D. Thorpe, C.T. Buckley, T. Vinardell, F.J. O'Brien, V.A. Campbell, D.J. Kelly, The response of bone marrow-derived mesenchymal stem cells to dynamic compression following tgf-β3 induced chondrogenic differentiation, Ann. Biomed. Eng. 38 (2010) 2896–2909, https://doi.org/10.1007/s10439-010-0059-6.

[29] A.E. Ryan, P. Lohan, L. O'Flynn, O. Treacy, X. Chen, C. Coleman, G. Shaw, M. Murphy, F. Barry, M.D. Griffin, T. Ritter, Chondrogenic differentiation increases antidonor immune response to allogeneic mesenchymal stem cell transplantation, Mol. Ther. 22 (2014) 655–667, https://doi.org/10.1038/mt.2013.261.

[30] D. Kouroupis, A.C. Bowles, M.A. Willman, C. Perucca Orfei, A. Colombini, T.M. Best, L.D. Kaplan, D. Correa, Infrapatellar fat pad-derived MSC response to inflammation and fibrosis induces an immunomodulatory phenotype involving CD10-mediated Substance P degradation, Sci. Rep. 9 (2019) 10864, https://doi.org/10.1038/s41598-019-47391-2.

[31] J.R. Steadman, K.K. Briggs, J.J. Rodrigo, M.S. Kocher, T.J. Gill, W.G. Rodkey, Outcomes of microfracture for traumatic chondral defects of the knee: average 11-year follow-up, Arthrosc. J. Arthrosc. Relat. Surg. 19 (2003) 477–484, https://doi.org/10.1053/jars.2003.50112.

[32] G.P. Doner, F.R. Noyes, Arthroscopic resection of fat pad lesions and infrapatellar contractures, Arthrosc. Tech. 3 (2014), https://doi.org/10.1016/j.eats.2014.04.002 e413–e416.

[33] H.V. Almeida, G.M. Cunniffe, T. Vinardell, C.T. Buckley, F.J. O'Brien, D.J. Kelly, Coupling freshly isolated CD44+ infrapatellar fat pad-derived stromal cells with a TGF-β3 eluting cartilage ECM-derived scaffold as a single-stage strategy for promoting chondrogenesis, Adv. Healthc. Mater. 4 (2015) 1043–1053, https://doi.org/10.1002/adhm.201400687.

[34] S. Huang, X. Song, T. Li, J. Xiao, Y. Chen, X. Gong, W. Zeng, L. Yang, C. Chen, Pellet coculture of osteoarthritic chondrocytes and infrapatellar fat pad-derived mesenchymal stem cells with chitosan/hyaluronic acid nanoparticles promotes chondrogenic differentiation, Stem Cell Res. Ther. 8 (2017) 264, https://doi.org/10.1186/s13287-017-0719-7.

[35] L. Bian, D.Y. Zhai, R.L. Mauck, J.A. Burdick, Coculture of human mesenchymal stem cells and articular chondrocytes reduces hypertrophy and enhances functional properties of engineered cartilage, Tissue Eng. 17 (2011) 1137–1145, https://doi.org/10.1089/ten.tea.2010.0531.

[36] X. Lv, G. Zhou, X. Liu, H. Liu, J. Chen, K. Liu, Y. Cao, Chondrogenesis by Co-culture of adipose-derived stromal cells and chondrocytes in vitro, Connect, Tissue Res 53 (2012) 492–497, https://doi.org/10.3109/03008207.2012.694926.

[37] T. Guo, J. Lembong, L.G. Zhang, J.P. Fisher, Three-dimensional printing articular cartilage: recapitulating the complexity of native tissue, Tissue Eng. B Rev. 23 (2017) 225–236, https://doi.org/10.1089/ten.teb.2016.0316.

[38] J. Fischer, A. Dickhut, M. Rickert, W. Richter, Human articular chondrocytes secrete parathyroid hormone-related protein and inhibit hypertrophy of mesenchymal stem cells in coculture during chondrogenesis, Arthritis Rheum. 62 (2010) 2696–2706, https://doi.org/10.1002/art.27565.

[39] L. Wu, H.J. Prins, M.N. Helder, C.A. Van Blitterswijk, M. Karperien, Trophic effects of mesenchymal stem cells in chondrocyte Co-Cultures are independent of culture conditions and cell sources, Tissue Eng. 18 (2012) 1542–1551, https://doi.org/10.1089/ten.tea.2011.0715.

[40] V.V. Meretoja, R.L. Dahlin, F.K. Kasper, A.G. Mikos, Enhanced chondrogenesis in co-cultures with articular chondrocytes and mesenchymal stem cells, Biomaterials 33 (2012) 6362–6369, https://doi.org/10.1016/j.biomaterials.2012.05.042.

[41] M.G. Haugh, C.M. Murphy, R.C. McKiernan, C. Altenbuchner, F.J. O'Brien, Crosslinking and mechanical properties significantly influence cell attachment, proliferation, and migration within collagen glycosaminoglycan scaffolds, Tissue Eng. 17 (2011) 1201–1208, https://doi.org/10.1089/ten.tea.2010.0590.

[42] J.P. Gleeson, N.A. Plunkett, F.J. O'Brien, Addition of hydroxyapatite improves stiffness, interconnectivity and osteogenic potential of a highly porous collagen-based scaffold for bone tissue regeneration, Eur. Cell. Mater. 20 (2010) 218–230, https://doi.org/10.22203/eCM.v020a18.

[43] C.J. Moran, A. Ramesh, P.A.J. Brama, J.M. O'Byrne, F.J. O'Brien, T.J. Levingstone, The benefits and limitations of animal models for translational research in cartilage repair, J. Exp. Orthop. 3 (2016), https://doi.org/10.1186/s40634-015-0037-x.

[44] M. Ahearne, Y. Liu, D.J. Kelly, Combining freshly isolated chondroprogenitor cells from the infrapatellar fat pad with a growth factor delivery hydrogel as a putative single stage therapy for articular cartilage repair, Tissue Eng. 20 (2014) 930–939, https://doi.org/10.1089/ten.tea.2013.0267.

[45] H.V. Almeida, Y. Liu, G.M. Cunniffe, K.J. Mulhall, A. Matsiko, C.T. Buckley, F.J. O'Brien, D.J. Kelly, Controlled release of transforming growth factor-β3 from cartilage-extra-cellular-matrix-derived scaffolds to promote chondrogenesis of human-joint-tissue-derived stem cells, Acta Biomater. 10 (2014) 4400–4409, https://doi.org/10.1016/j.actbio.2014.05.030.

[46] C.M. Murphy, A. Schindeler, J.P. Gleeson, N.Y.C. Yu, L.C. Cantrill, K. Mikulec, L. Peacock, F.J. O'Brien, D.G. Little, A collagen-hydroxyapatite scaffold allows for binding and co-delivery of recombinant bone morphogenetic proteins and

bisphosphonates, Acta Biomater. 10 (2014) 2250–2258, https://doi.org/10.1016/j.actbio.2014.01.016.
[47] M. Sartori, S. Pagani, A. Ferrari, V. Costa, V. Carina, E. Figallo, M.C. Maltarello, L. Martini, M. Fini, G. Giavaresi, A new bi-layered scaffold for osteochondral tissue regeneration: in vitro and in vivo preclinical investigations, Mater. Sci. Eng. C 70 (2017) 101–111, https://doi.org/10.1016/j.msec.2016.08.027.
[48] B.P. Chan, T.Y. Hui, M.Y. Wong, K.H.K. Yip, G.C.F. Chan, Mesenchymal stem cell-encapsulated collagen microspheres for bone tissue engineering, Tissue Eng. C Methods 16 (2010) 225–235, https://doi.org/10.1089/ten.tec.2008.0709.
[49] R. Mishra, A. Kumar, Osteocompatibility and osteoinductive potential of supermacroporous polyvinyl alcohol-TEOS-Agarose-CaCl2 (PTAgC) biocomposite cryogels, J. Mater. Sci. Mater. Med. 25 (2014) 1327–1337, https://doi.org/10.1007/s10856-014-5166-8.
[50] V. Irawan, T.C. Sung, A. Higuchi, T. Ikoma, Collagen scaffolds in cartilage tissue engineering and relevant approaches for future development, Tissue Eng. Regen. Med. 15 (2018) 673–697, https://doi.org/10.1007/s13770-018-0135-9.
[51] S.M. Becerra-Bayona, V.R. Guiza-Arguello, B. Russell, M. Höök, M.S. Hahn, Influence of collagen-based integrin α1 and α2 mediated signaling on human mesenchymal stem cell osteogenesis in three dimensional contexts, J. Biomed. Mater. Res. 106 (2018) 2594–2604, https://doi.org/10.1002/jbm.a.36451.
[52] R.M. Salasznyk, W.A. Williams, A. Boskey, A. Batorsky, G.E. Plopper, Adhesion to vitronectin and collagen I promotes osteogenic differentiation of human mesenchymal stem cells, J. Biomed. Biotechnol. 2004 (2004) 24–34, https://doi.org/10.1155/S1110724304306017.
[53] M. Mizuno, R. Fujisawa, Y. Kuboki, Type I collagen-induced osteoblastic differentiation of bone-marrow cells mediated by collagen-α2β1 integrin interaction, J. Cell. Physiol. 184 (2000) 207–213, https://doi.org/10.1002/1097-4652(200008)184:2<207::AID-JCP8>3.0.CO;2.
[54] F.G. Lyons, A.A. Al-Munajjed, S.M. Kieran, M.E. Toner, C.M. Murphy, G.P. Duffy, F.J. O'Brien, The healing of bony defects by cell-free collagen-based scaffolds compared to stem cell-seeded tissue engineered constructs, Biomaterials 31 (2010) 9232–9243, https://doi.org/10.1016/j.biomaterials.2010.08.056.
[55] F. Viti, M. Landini, A. Mezzelani, L. Petecchia, L. Milanesi, S. Scaglione, Osteogenic differentiation of MSC through calcium signaling activation: transcriptomics and functional analysis, PLoS One 11 (2016), e0148173, https://doi.org/10.1371/journal.pone.0148173.
[56] C.M. Murphy, A. Matsiko, M.G. Haugh, J.P. Gleeson, F.J. O'Brien, Mesenchymal stem cell fate is regulated by the composition and mechanical properties of collagen-glycosaminoglycan scaffolds, J. Mech. Behav. Biomed. Mater. 11 (2012) 53–62, https://doi.org/10.1016/j.jmbbm.2011.11.009.
[57] A.J. Engler, S. Sen, H.L. Sweeney, D.E. Discher, Matrix elasticity directs stem cell lineage specification, Cell 4 (2006) 677–689, https://doi.org/10.1016/j.cell.2006.06.044.
[58] P. Orth, M. Cucchiarini, G. Kaul, M.F. Ong, S. Gräber, D.M. Kohn, H. Madry, Temporal and spatial migration pattern of the subchondral bone plate in a rabbit osteochondral defect model, Osteoarthritis Cartilage 20 (2012) 1161–1169, https://doi.org/10.1016/j.joca.2012.06.008.
[59] Y.S. Qui, B.F. Shahgaldi, W.J. Revell, F.W. Heatley, Observations of subchondral plate advancement during osteochondral repair: a histomorphometric and mechanical study in the rabbit femoral condyle, Osteoarthritis Cartilage 11 (2003) 810–820, https://doi.org/10.1016/S1063-4584(03)00164-X.
[60] T. Minas, A.H. Gomoll, R. Rosenberger, R.O. Royce, T. Bryant, Increased failure rate of autologous chondrocyte implantation after previous treatment with marrow stimulation techniques, Am. J. Sports Med. 37 (2009) 902–908, https://doi.org/10.1177/0363546508330137.
[61] P.C. Kreuz, M.R. Steinwachs, C. Erggelet, S.J. Krause, G. Konrad, M. Uhl, N. Südkamp, Results after microfracture of full-thickness chondral defects in different compartments in the knee, Osteoarthritis Cartilage 14 (2006) 1119–1125, https://doi.org/10.1016/j.joca.2006.05.003.
[62] T. Furukawa, D.R. Eyre, S. Koide, M.J. Glimcher, Biochemical studies on repair cartilage resurfacing experimental defects in the rabbit knee, J. Bone Jt. Surg. - Ser. A. 62 (1980) 79–89, https://doi.org/10.2106/00004623-198062010-00012.
[63] S.P. Nukavarapu, D.L. Dorcemus, Osteochondral tissue engineering: current strategies and challenges, Biotechnol. Adv. 31 (2013) 706–721, https://doi.org/10.1016/j.biotechadv.2012.11.004.
[64] E. Farrell, F.J. O'Brien, P. Doyle, J. Fischer, I. Yannas, B.A. Harley, B. O'Connell, P.J. Prendergast, V.A. Campbell, A collagen-glycosaminoglycan scaffold supports adult rat mesenchymal stem cell differentiation along osteogenic and chondrogenic routes, Tissue Eng. 12 (2006) 459–468, https://doi.org/10.1089/ten.2006.12.459.
[65] M. Rutgers, D.B. Saris, L.A. Vonk, M.H. Van Rijen, V. Akrum, D. Langeveld, A. Van Boxtel, W.J. Dhert, L.B. Creemers, Effect of collagen type I or type II on chondrogenesis by cultured human articular chondrocytes, Tissue Eng. 19 (2013) 59–65, https://doi.org/10.1089/ten.tea.2011.0416.
[66] M. Tamaddon, M. Burrows, S.A. Ferreira, F. Dazzi, J.F. Apperley, A. Bradshaw, D.D. Brand, J. Czernuszka, E. Gentleman, Monomeric, porous type II collagen scaffolds promote chondrogenic differentiation of human bone marrow mesenchymal stem cells in vitro, Sci. Rep. 7 (2017) 43519, https://doi.org/10.1038/srep43519.
[67] E. Amann, P. Wolff, E. Breel, M. van Griensven, E.R. Balmayor, Hyaluronic acid facilitates chondrogenesis and matrix deposition of human adipose derived mesenchymal stem cells and human chondrocytes co-cultures, Acta Biomater. 52 (2017) 130–144, https://doi.org/10.1016/j.actbio.2017.01.064.
[68] M.L. Vainieri, A. Lolli, N. Kops, D. D'Atri, D. Eglin, A. Yayon, M. Alini, S. Grad, K. Sivasubramaniyan, G.J.V.M. van Osch, Evaluation of biomimetic hyaluronic-based hydrogels with enhanced endogenous cell recruitment and cartilage matrix formation, Acta Biomater. 101 (2020) 293–303, https://doi.org/10.1016/j.actbio.2019.11.015.
[69] A. Matsiko, T.J. Levingstone, F.J. O'Brien, J.P. Gleeson, Addition of hyaluronic acid improves cellular infiltration and cartilage-specific extracellular matrix synthesis in a porous collagen scaffold, Eur. Cell. Mater. 20 (2010).
[70] J. Li, S. Mareddy, D.M. Tan, R. Crawford, X. Long, X. Miao, Y. Xiao, A minimal common osteochondrocytic differentiation medium for the osteogenic and chondrogenic differentiation of bone marrow stromal cells in the construction of osteochondral graft, Tissue Eng. 15 (2009) 2481–2490, https://doi.org/10.1089/ten.tea.2008.0463.
[71] D.L. Dorcemus, E.O. George, C.N. Dealy, S.P. Nukavarapu, Harnessing external cues: development and evaluation of an in vitro culture system for osteochondral tissue engineering, Tissue Eng. 23 (2017) 719–737, https://doi.org/10.1089/ten.tea.2016.0439.
[72] J. Li, Y.-C. Chen, Y.-C. Tseng, S. Mozumdar, L. Huang, Biodegradable calcium phosphate nanoparticle with lipid coating for systemic siRNA delivery, J. Contr. Release 142 (2010) 416–421, https://doi.org/10.1016/j.jconrel.2009.11.008.
[73] L. Peterson, H.S. Vasiliadis, M. Brittberg, A. Lindahl, Autologous chondrocyte implantation: a long-term follow-up, Am. J. Sports Med. 38 (2010) 1117–1124, https://doi.org/10.1177/0363546509357915.
[74] Y. Liu, C.T. Buckley, H.V. Almeida, K.J. Mulhall, D.J. Kelly, Infrapatellar fat pad-derived stem cells maintain their chondrogenic capacity in disease and can be used to engineer cartilaginous grafts of clinically relevant dimensions, Tissue Eng. 20 (2014) 3050–3062, https://doi.org/10.1089/ten.tea.2014.0035.
[75] Y. Han, H. Li, R. Zhou, J. Wu, Z. Liu, H. Wang, J. Shao, Y. Chen, J. Zhu, Q. Fu, Q. Qian, Y. Zhou, Comparison between intra-articular injection of infrapatellar fat pad (IPFP) cell concentrates and IPFP-mesenchymal stem cells (MSCs) for cartilage defect repair of the knee joint in rabbits, Stem Cell. Int. 2021 (2021), https://doi.org/10.1155/2021/9966966.
[76] F.S. Toghraie, N. Chenari, M.A. Gholipour, Z. Faghih, S. Torabinejad, S. Dehghani, A. Ghaderi, Treatment of osteoarthritis with infrapatellar fat pad derived mesenchymal stem cells in Rabbit, Knee 18 (2011) 71–75, https://doi.org/10.1016/j.knee.2010.03.001.
[77] B.J. Huang, D.J. Huey, J.C. Hu, K.A. Athanasiou, Engineering biomechanically functional neocartilage derived from expanded articular chondrocytes through the manipulation of cell-seeding density and dexamethasone concentration, J. Tissue Eng. Regen. Med. 11 (2017) 2323–2332, https://doi.org/10.1002/term.2132.
[78] C.B. Foldager, A.H. Gomoll, M. Lind, M. Spector, Cell seeding densities in autologous chondrocyte implantation techniques for cartilage repair, Cartilage 3 (2012) 108–117, https://doi.org/10.1177/1947603511435522.
[79] S. Talukdar, Q.T. Nguyen, A.C. Chen, R.L. Sah, S.C. Kundu, Effect of initial cell seeding density on 3D-engineered silk fibroin scaffolds for articular cartilage tissue engineering, Biomaterials 32 (2011) 8927–8937, https://doi.org/10.1016/j.biomaterials.2011.08.027.
[80] R.J.F.C. Do Amaral, H.V. Almeida, D.J. Kelly, F.J. O'Brien, C.J. Kearney, Infrapatellar fat pad stem cells: from developmental biology to cell therapy, Stem Cell. Int. (2017) 6843727, https://doi.org/10.1155/2017/6843727, 2017.
[81] C. Acharya, A. Adesida, P. Zajac, M. Mumme, J. Riesle, I. Martin, A. Barbero, Enhanced chondrocyte proliferation and mesenchymal stromal cells chondrogenesis in coculture pellets mediate improved cartilage formation, J. Cell. Physiol. 227 (2012) 88–97, https://doi.org/10.1002/jcp.22706.